

The topology of Gelfand–Zeitlin fibers

Jeffrey D. Carlson and Jeremy Lane

January 13, 2022

Abstract

We prove several new results about the topology of fibers of Gelfand–Zeitlin systems on unitary and orthogonal coadjoint orbits. First, we provide a simplified description of their diffeomorphism types as balanced products, recovering results of Bouloc–Miranda–Zung as special cases. Second, we compute their cohomology rings. Finally, we complete the computation of their first three homotopy groups (the first and second homotopy groups were described by Cho–Kim–Oh in the unitary case). Our results build on Cho–Kim–Oh’s description of Gelfand–Zeitlin fibers as total spaces of certain towers of fiber bundles. Our description of the diffeomorphism type, cohomology ring, and homotopy groups can be read in a straightforward manner from the combinatorics of the associated Gelfand–Zeitlin pattern.

1. Introduction

Gelfand–Zeitlin systems are a family of completely integrable systems named for their connection to Gelfand–Zeitlin canonical bases [GS83a],¹ most commonly studied on coadjoint orbits of unitary and orthogonal Lie groups. The fibers of their moment maps, or *Gelfand–Zeitlin fibers*, are interesting from several perspectives, such as geometric quantization [GS83a, HK14], Floer theory [NNU10, NU16, CKO20], and the topology of integrable systems on symplectic manifolds [BMMT18, Problem 2.9]. The moment map images of Gelfand–Zeitlin systems on unitary and orthogonal coadjoint orbits are polytopes known as *Gelfand–Zeitlin polytopes* whose faces are enumerated by combinatorial diagrams called *Gelfand–Zeitlin patterns*² (see Figure 4). The Gelfand–Zeitlin (henceforth GZ) fiber over a given point is naturally associated with the GZ pattern of the face of the GZ polytope containing the point in its relative interior.

In recent work, Cho, Kim and Oh observed that both unitary and orthogonal GZ fibers are total spaces of certain towers of fiber bundles [CKO20, CK20]. They used this description to show that every unitary GZ fiber decomposes as a direct product of a torus and a space whose first and second homotopy groups are trivial. They were also able to explicitly describe the fibers in each stage of their towers as certain products of spheres determined by the combinatorics of the associated pattern. In particular, their results give a combinatorial formula for the dimension of a fiber in terms of the associated pattern. Unitary GZ fibers were also studied by Bouloc, Miranda, and Zung from a very different perspective [BouMZ18]. In addition to recovering an equivalent dimension counting formula, they show that every unitary GZ fiber admits a product decomposition, finer than Cho–Kim–Oh’s, in which direct factors are enumerated by connected components of the associated GZ pattern. In the case where a connected component is a diamond, they are

¹ The name “Zeitlin” is variously romanized in the literature, also appearing as “Cetlin” and “Tsetlin.”

² Some authors prefer to use ladder diagrams, which are equivalent.

able to simplify their description of the corresponding factor to show that it is diffeomorphic to a unitary group.

Although these recent results have greatly improved our understanding of GZ fibers, they do not provide a clear description of the topology of GZ fibers in all cases. For example, it is not clear how to extract from these results a simple, useful description of the diffeomorphism type of the GZ fiber corresponding to more complicated patterns such as that of Figure 4. This brings us to our first result. We use Cho–Kim–Oh’s towers to show that every unitary and orthogonal GZ fiber can be expressed as a balanced product, that is, a quotient of the form

$$\begin{aligned} & H_a \times H_{a+1} \times \cdots \times H_n / L_a \times L_{a+1} \times \cdots \times L_n, \\ & (h_a, h_{a+1}, \dots, h_n) \sim (h_a \ell_a^{-1}, \psi_a(\ell_a) h_{a+1} \ell_{a+1}^{-1}, \dots, \psi_{n-1}(\ell_{n-1}) h_n \ell_n^{-1}), \end{aligned} \tag{1.1}$$

where the groups H_k and L_k are certain products of unitary and orthogonal groups determined by the GZ pattern and $\psi_k: L_k \rightarrow H_{k+1}$ are certain injective homomorphisms (see Theorem 3.2). It follows immediately from this description that every GZ fiber is a direct product whose factors correspond to connected components of the GZ pattern, a result which is new in the orthogonal case (see Corollary 3.3). More importantly, we are able to systematically simplify the expressions (1.1) in terms of the combinatorics of the associated GZ pattern. As a result of this systematic simplification, we are able to provide relatively simple descriptions of the diffeomorphism types of all GZ fibers, even those with relatively complex GZ patterns such as in Figure 4 (see Example 1.3 below). We illustrate these results with a number of examples (Examples 3.11–3.18). In particular, our results recover the descriptions of elliptic non-degenerate singular fibers and multi-diamond singular fibers given by Bouloc *et al.* as special cases. We also observe that the quotients (1.1) can be described as biquotients (Theorem 3.8).

For our second result, we compute the cohomology rings of arbitrary fibers of GZ systems on arbitrary coadjoint orbits of unitary and orthogonal Lie groups. For the sake of the introduction, we summarize these results in the following.

Theorem 1.2. *The integral cohomology of a unitary Gelfand–Zeitlin fiber is an exterior algebra on odd-degree generators. The cohomology of an orthogonal Gelfand–Zeitlin fiber over $\mathbb{Z}[1/2]$ is also an exterior algebra; the integral and mod-2 cohomology groups are isomorphic to those of a product of real Stiefel manifolds.*

The degrees of the relevant generators and the precise relevant Stiefel manifolds are again determined in a straightforward manner from the associated GZ pattern; see Theorems 4.1 and 5.11 for more details. These cohomology computations follow inductively from an analysis of the Serre spectral sequences associated to Cho–Kim–Oh’s towers. Surprisingly, the spectral sequence associated to each bundle collapses in the unitary case, and moreover, as the cohomology of base and fiber for each bundle are exterior algebras, there is no extension problem, additively or multiplicatively. In the orthogonal case, the spectral sequences do not necessarily collapse, but through a somewhat more complicated analysis we are able to extract the integral cohomology groups and to show once the torsion ideal is quotiented out of the integral cohomology ring, the resulting algebra is again exterior.

Finally, we study the homotopy groups of Gelfand–Zeitlin fibers. We observe that orthogonal fibers split as a product of a torus and a space whose first and second homotopy groups have the form $(\mathbb{Z}/2)^s$ and \mathbb{Z}^f respectively. We also show that the third homotopy groups of unitary and orthogonal GZ fibers are free abelian. See Propositions 4.7 and 5.20.

Example 1.3. Consider the GZ pattern in Figure 4. Using our results, one can immediately read from this pattern that an associated GZ fiber is diffeomorphic to

$$(S^1)^7 \times (S^3)^3 \times \mathrm{U}(2) \backslash (\mathrm{U}(4) \times \mathrm{U}(3)) / \mathrm{U}(2),$$

has integral cohomology ring isomorphic to

$$\Lambda[z_{1,1}, z_{1,2}, z_{1,3}, z_{1,4}, z_{1,5}, z_{1,6}, z_{1,7}, z_{3,1}, z_{5,1}, z_{5,2}, z_{7,1}], \quad |z_{m,j}| = m,$$

and has $\pi_3 \cong \mathbb{Z}^3$. See Examples 3.18 and 4.2 for more details.

We end this introduction with a discussion of the broader context and motivation for our work. Gelfand–Zeitlin systems are useful because they share many features with toric integrable systems (convexity and global action-angle coordinates) but they are interesting because they have non-toric singularities. In fact, GZ systems are part of a larger family of examples with similar behaviour that also includes bending flow systems on polygon space [KapM96], Goldman systems on moduli space [Gold86], and integrable systems constructed by toric degeneration [HK15] (of which GZ systems are an example [NNU10]). This larger family of examples is growing. For instance, the construction of integrable systems by toric degeneration was recently extended [HL20], and as a consequence, it was shown that every coadjoint orbit of every compact, connected Lie group admits integrable systems that share the features of GZ systems mentioned above.

There are many questions regarding the non-toric singularities of these integrable systems which are currently unanswered. For example, it is known in the cases of bending flow systems [Bou18] and GZ systems [BouMZ18, CKO20] that the non-toric fibers are isotropic (this result is expected to have applications in Lagrangian Floer theory [CKO20]), but it is not known whether non-toric fibers of integrable systems constructed by toric degeneration are isotropic in general (this was conjectured to be true by Bouloc *et al.* [BouMZ18]). Similarly, very little is known in general about the topology of non-toric fibers of integrable systems constructed by toric degeneration. There is also the problem of finding local normal forms for the non-toric singularities of these systems, as motivated by Bolsinov *et al.* for the case of GZ systems [BMMT18, Problem 2.9]. At the moment, very little is known about this problem, even in the case of the more concrete GZ systems, with the exception of several examples in low dimension studied by Alamiddine [Ala09]. Progress on any of these questions would have further applications in symplectic topology, geometric quantization, and the topology of integrable systems.

To give a particularly concrete example of one such application, we end by describing one of the original motivations for studying GZ systems (and a potential future application of this work). Guillemin and Sternberg observed that if integral points in the boundary of an integral GZ polytope are formally included in the Bohr–Sommerfeld set, then the dimension of the resulting Bohr–Sommerfeld quantization equals the dimension of the Kähler quantization of the coadjoint orbit [GS83a]. In ongoing work, we plan to use our description of the topology of the singular GZ fibers, and a description of a local model for the GZ systems in neighbourhoods of said fibers, to give a more principled justification of Guillemin and Sternberg’s observation, i.e., to prove that a singular fiber is Bohr–Sommerfeld if and only if it is integral. Moreover, we hope to extend the results of Hamilton–Kono [HK14] by showing that holomorphic sections in the Kähler quantization that correspond to boundary points of the GZ polytope converge under a deformation of complex structure to distributional sections supported on the singular fibers over the same boundary points.

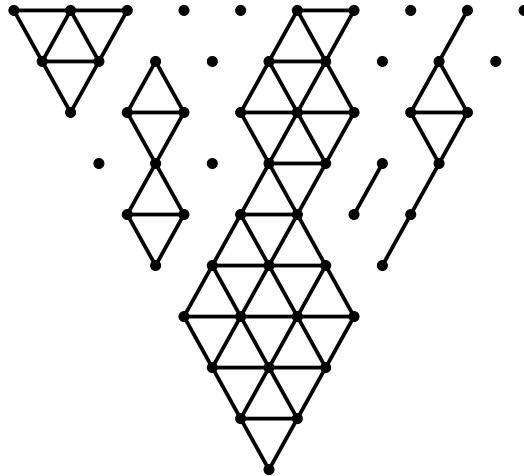


Figure 4: Example of a GZ pattern associated to a fiber of a GZ system on a non-regular coadjoint orbit of $U(10)$.

Organization of the paper. In Section 2, we recall the description of GZ fibers as towers. In particular, we recall results of Cho–Kim–Oh which describe the bundles of homogeneous spaces that occur at each stage in terms of the associated GZ pattern [CKO20, CK20]. We note a minor correction to Cho and Kim’s description [CK20] of the bundles in the orthogonal case (although this correction does not impact their final results, it does play an important role in our cohomology computations). Section 3 contains our description of the GZ fibers as biquotients (Theorem 3.8). It also shows that GZ fibers decompose as direct products (a result which is new in the orthogonal case). We provide examples demonstrating how easily our biquotient description can be read from the associated GZ pattern. In Section 4, we state and prove the main theorem (Theorem 4.1) regarding cohomology of GZ fibers in the unitary case. Finally, Section 5 contains our cohomological results in the orthogonal case. We conclude with a remark comparing our proof with a general expression for the cohomology of a biquotient.

Acknowledgements. Both authors were supported by a Fields Postdoctoral Fellowship associated with the 2020 Thematic Program in Toric Topology during the original collaborative work that lead to this manuscript.

2. Gelfand–Zeitlin systems and Gelfand–Zeitlin fibers

This section recalls the Gelfand–Zeitlin systems on unitary and orthogonal coadjoint orbits as well as the description of their fibers as towers. In order to avoid repeating ourselves, we begin in Section 2.1 by giving a general description of GZ systems and fibers that applies equally in both cases. We recall the details that are specific to the unitary and orthogonal cases in Sections 2.2 and 2.3 respectively.

For further details regarding GZ systems, we direct the reader to the original papers of Guillemin and Sternberg [GS83a, GS83b] and the recent papers of Cho–Kim–Oh describing the GZ fibers as towers of bundles of homogeneous spaces [CK20, CKO20]. As mentioned in the introduction, an alternative description of the GZ fibers is given by Bouloc *et al.* [BouMZ18]. We also remark that the Ph.D. thesis of Milena Pabiniak [Pab12] contains many useful details.

2.1. The general case

This section shows how GZ fibers of both unitary and orthogonal GZ systems are towers of bundles of homogeneous spaces in terms of a somewhat more general set-up.

Notation 2.1. Fix positive integers $a < n$ and let G_k ($a \leq k \leq n+1$) be compact, connected Lie groups with Lie algebras \mathfrak{g}_k . For each k , fix a maximal torus T_k in each G_k , denoting its Lie algebra by \mathfrak{t}_k , and fix positive Weyl chambers $\mathfrak{t}_{k,+}^*$ in the linear duals \mathfrak{t}_k^* . We identify \mathfrak{t}_k^* in the standard way with the fixed points of \mathfrak{g}_k^* under the coadjoint action of T_k . We will write $\lambda^{(k)}$ for points of $\mathfrak{t}_{k,+}^*$. We denote by $\mathcal{S}_k: \mathfrak{g}_k^* \rightarrow \mathfrak{t}_k^*$ the continuous map that sends an element $\zeta \in \mathfrak{g}_k^*$ to the unique element $\lambda^{(k)} \in \mathfrak{t}_{k,+}^*$ lying in its coadjoint G_k -orbit $\mathcal{O}_{\lambda^{(k)}} = G_k \cdot \zeta$.

Fix a sequence of Lie group homomorphisms $\varphi_k: G_k \rightarrow G_{k+1}$ ($a \leq k \leq n+1$). From the induced maps $\varphi_k^*: \mathfrak{g}_{k+1}^* \rightarrow \mathfrak{g}_k^*$ of cotangent spaces and the maps \mathcal{S}_k , we can associate to each point $\lambda^{(n+1)} \in \mathfrak{t}_{+,n+1}^*$ a map

$$\begin{aligned} \Psi: \mathcal{O}_{\lambda^{(n+1)}} &\longrightarrow \mathfrak{t}_n^* \times \cdots \times \mathfrak{t}_a^*, \\ \Psi &:= (\mathcal{S}_n \circ \varphi_n^*, \mathcal{S}_{n-1} \circ \varphi_{n-1}^* \circ \varphi_n^*, \dots, \mathcal{S}_a \circ \varphi_a^* \circ \cdots \circ \varphi_n^*) \end{aligned} \quad (2.2)$$

extracting for each $\zeta \in \mathcal{O}_{\lambda^{(n+1)}}$ and each k the point of $\mathfrak{t}_{k,+}^*$ lying in the coadjoint orbit of the image $(\varphi_k^* \circ \cdots \circ \varphi_n^*)(\zeta)$. The map Ψ generates a Hamiltonian action of $T_n \times \cdots \times T_a$ on an open, dense subset of $\mathcal{O}_{\lambda^{(n+1)}}$, with respect to the canonical Kostant–Kirillov–Souriau symplectic structure on $\mathcal{O}_{\lambda^{(n+1)}}$ [GS83a]. It was shown in a more general setting by the second author that the dense subset where Ψ generates a torus action is connected and the fibers of Ψ are all connected [Lane18].

In the following subsections, we will describe two families of examples of the setup above. In both cases, the resulting densely defined torus action is completely integrable, or toric, for every $\lambda^{(n+1)}$ in $\mathfrak{t}_{+,n+1}^*$. In these cases, the map Ψ is called a *Gelfand–Zeitlin (GZ) system* and each fiber $\Psi^{-1}(\lambda^{(n)}, \dots, \lambda^{(a)})$ a *Gelfand–Zeitlin (GZ) fiber*.

Note that as φ_k^* is G_k -equivariant, G_k acts upon each nonempty intersection

$$\mathcal{O}_{\lambda^{(k+1)}, \lambda^{(k)}} := (\varphi_k^*)^{-1}(\mathcal{O}_{\lambda^{(k)}}) \cap \mathcal{O}_{\lambda^{(k+1)}}$$

via the homomorphism φ_k and the coadjoint action of G_{k+1} . In the specific case of the unitary and orthogonal GZ systems (where the set-up is fixed as in the two subsections which follow), the G_k -action on each non-empty set $\mathcal{O}_{\lambda^{(k+1)}, \lambda^{(k)}}$ is transitive [GS83b]. This special property is crucial for the interpretation which we now give of the fibers of Ψ as the total spaces of certain towers.

If we fix $\lambda^{(n+1)}, \lambda^{(n)}, \dots, \lambda^{(a)}$ such that $\Psi^{-1}(\lambda^{(n)}, \dots, \lambda^{(a)})$ is a non-empty fiber of a GZ system on $\mathcal{O}_{\lambda^{(n+1)}}$, then for all $a \leq k \leq n$, both $\mathcal{O}_{\lambda^{(k+1)}, \lambda^{(k)}}$ and $\mathcal{O}_{\lambda^{(k)}}$ are homogeneous G_k -spaces, and the G_k -equivariant map $\varphi_k^*: \mathfrak{g}_{k+1}^* \rightarrow \mathfrak{g}_k^*$ restricts to a bundle projection $\pi_k: \mathcal{O}_{\lambda^{(k+1)}, \lambda^{(k)}} \rightarrow \mathcal{O}_{\lambda^{(k)}}$. Pulling back these bundles via the inclusions $\iota_k: \mathcal{O}_{\lambda^{(k+1)}, \lambda^{(k)}} \hookrightarrow \mathcal{O}_{\lambda^{(k+1)}}$ results in a large diagram in which $F_k^k = \mathcal{O}_{\lambda^{(k)}}$, $F_k^{k+1} = \mathcal{O}_{\lambda^{(k+1)}, \lambda^{(k)}}$, the maps $F_k^{k+1} \rightarrow F_{k+1}^{k+1}$ are ι_k , the maps $F_k^{k+1} \rightarrow F_k^k$ are π_k , for each k , and the other spaces and maps are defined so that each square is a pullback. Since G_a is a torus, F_a^a is a point. As each pullback imposes an additional restriction on the long vertical compositions $\varphi_k^* \circ \cdots \circ \varphi_n^*$ in Figure 3, the space F_a^{n+1} in the upper left corner is the GZ fiber $\Psi^{-1}(\lambda^{(n)}, \dots, \lambda^{(a)})$.

In order to compute the cohomology of the GZ fibers, it will help to give π_k , ι_k , and Figure 3 slightly different descriptions. Let $H_k \leq G_k$ denote the stabilizer of $\lambda^{(k)}$ with respect to the coadjoint action of G_k and fix a point ζ_k in $\mathcal{O}_{\lambda^{(k+1)}, \lambda^{(k)}}$, letting $L_k \leq H_k$ denote its stabilizer. This choice

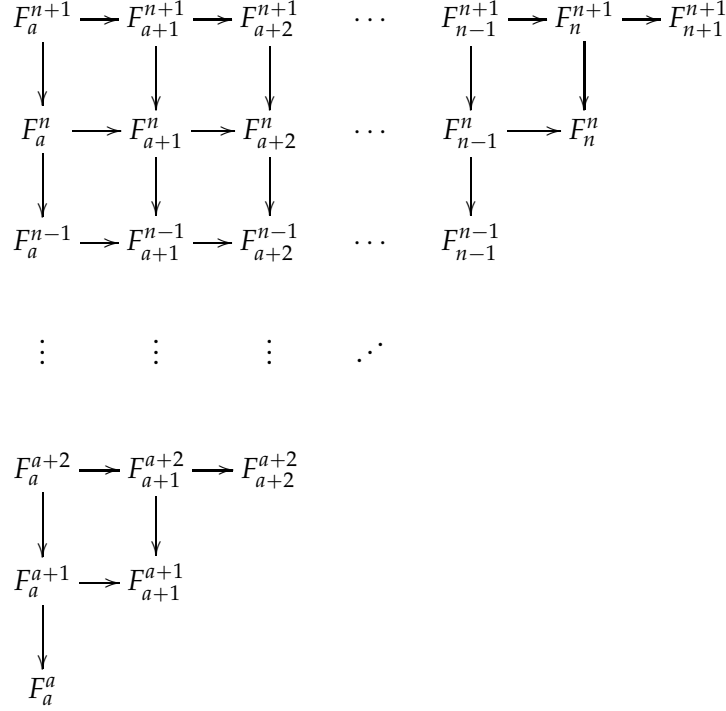


Figure 3: Gelfand–Zeitlin fibers can be viewed as the total space F_a^{n+1} of a tower of fiber bundles (on the left side of the diagram) which is constructed through a sequence of pullbacks.

of ξ_k fixes an identification of π_k with the projection map in the bundle of homogeneous spaces

$$H_k/L_k \rightarrow G_k/L_k \rightarrow G_k/H_k. \quad (2.4)$$

For any $A \in G_{k+1}$ such that $A\phi_k(L_k)A^{-1}$ is contained in H_{k+1} and for any $B \in G_{k+1}$, we define a composite map

$$\iota_{A,B}: \frac{G_k}{L_k} \hookrightarrow \frac{G_{k+1}}{\phi_k(L_k)} \longrightarrow \frac{G_{k+1}}{A\phi_k(L_k)A^{-1}} \twoheadrightarrow \frac{G_{k+1}}{H_{k+1}}. \quad (2.5)$$

The first map in this composition is the map induced by the homomorphism ϕ_k . The second map is the isomorphism of G_{k+1} -homogeneous spaces given by multiplication by B on the left and multiplication by A^{-1} on the right. In other words, for all $g \in G_{k+1}$, the middle map is

$$g\phi_k(L_k) \longmapsto Bg\phi_k(L_k)A^{-1} = BgA^{-1} \cdot A\phi_k(L_k)A^{-1}.$$

The last map is the natural projection. We record the following lemma which is straightforward and will be important in what follows.

Lemma 2.6. *Make identifications $\mathcal{O}_{\lambda^{(k+1)}, \lambda^{(k)}} \cong G_k/L_k$ and $\mathcal{O}_{\lambda^{(k+1)}} \cong G_{k+1}/H_{k+1}$ by fixing $\xi_k \in \mathcal{O}_{\lambda^{(k+1)}, \lambda^{(k)}}$ and $\lambda^{(k+1)} \in \mathcal{O}_{\lambda^{(k+1)}}$ as above, and let $A \in G_{k+1}$ be such that $\lambda^{(k+1)} = \text{Ad}_A^* \xi_k$. Then the embedding ι_k is identified with the composition $\iota_{A,1}$ of (2.5).*

Thus, we can reinterpret the diagram of Figure 3 as follows: the spaces F_k^k are G_k/H_k , the spaces F_k^{k+1} are G_k/L_k , the maps $F_k^{k+1} \rightarrow F_k^k$ are the bundle projections of (2.4), the maps $F_k^{k+1} \rightarrow F_{k+1}^{k+1}$ are embeddings $\iota_{A,B}$ as in (2.5) for some choice of $A, B \in G_{k+1}$ (2.5), and all other maps

are constructed by pullback. By Lemma 2.6, $A, B \in G_{k+1}$ can be chosen so that this diagram is identified with the previous description, given above.

Each map $\iota_{A,B}$ is equal to the composition of $\iota_{A,1}$ with left translation by B on the codomain G_{k+1}/H_{k+1} . Since left multiplication by B is an automorphism of the bundle $G_{k+1}/L_{k+1} \rightarrow G_{k+1}/H_{k+1}$, the pullbacks of this bundle by $\iota_{A,B}$ and $\iota_{A,1}$ are diffeomorphic. It follows that the resulting final pullbacks F_a^{n+1} in Figure 3 are diffeomorphic, regardless of the choice of elements $B \in G_{k+1}$ for each k . In particular, if we instead take $B = A$ for each k , the new F_a^{n+1} is diffeomorphic to the GZ fiber $\Psi^{-1}(\lambda^{(n)}, \dots, \lambda^{(a)})$, but the map $\iota_{A,A}$ has a simpler description as the map $gL_k \mapsto \psi_k(g)H_{k+1}$ of homogeneous spaces induced by the homomorphism $\psi_k: G_k \rightarrow G_{k+1}$ given by $g \mapsto A\varphi_k A^{-1}$. This description will be important starting with Theorem 3.2.

2.2. The unitary case

This section describes unitary GZ systems and their fibers as a special case of the set-up in the previous section. Since we have already given a general description of the GZ fibers in Figure 3, all that remains is to describe the groups $L_k \leq H_k \leq G_k$ that occur in this case.

For $k = 1, \dots, n+1$, let G_k be the group $U(k)$ of unitary $k \times k$ matrices and let T_k be the maximal torus of diagonal matrices in G_k . The coadjoint representation of G_k on \mathfrak{g}_k^* can be identified linearly with action of G_k by conjugation on the space of $k \times k$ skew-Hermitian matrices. The positive Weyl chambers $\mathfrak{t}_{k,+}^*$ can be identified with the set points $\lambda^{(k)} = (\lambda_1^{(k)}, \dots, \lambda_k^{(k)}) \in \mathbb{R}^k$ such that $\lambda_1^{(k)} \geq \dots \geq \lambda_k^{(k)}$. We make these identifications so that the coadjoint orbit $\mathcal{O}_{\lambda^{(k)}}$ is identified with the set of $k \times k$ skew-Hermitian matrices with eigenvalues $i\lambda_1^{(k)}, \dots, i\lambda_k^{(k)}$.

Although any choice of embeddings $\varphi_k: G_k \rightarrow G_{k+1}$ will do, for concreteness we fix $\varphi_k(g) = g \oplus [1]$, where $g \oplus [1] \in U(k+1)$ is the block diagonal matrix whose upper-left principal $k \times k$ submatrix is g and whose lower-right principal 1×1 submatrix is $[1]$. With these choices, the map Ψ defined in (2.2) is a GZ system on any coadjoint orbit $\mathcal{O}_{\lambda^{(n+1)}}$ of $U(n+1)$ [GS83b].

It is a result of linear algebra that $\mathcal{O}_{\lambda^{(k+1)}, \lambda^{(k)}}$ is non-empty if and only if $\lambda^{(k)}$ and $\lambda^{(k+1)}$ satisfy *interlacing inequalities*

$$\begin{array}{ccccccccc} \lambda_1^{(k+1)} & & \lambda_2^{(k+1)} & & \lambda_3^{(k+1)} & & \lambda_k^{(k+1)} & & \lambda_{k+1}^{(k+1)} \\ & \searrow & & \searrow & & \searrow & & \searrow & \\ & \lambda_1^{(k)} & & \lambda_2^{(k)} & & \dots & & \lambda_k^{(k)} & \end{array} \quad (2.7)$$

The image of the GZ system on $\mathcal{O}_{\lambda^{(n+1)}}$ is the set of those points in $\mathbb{R}^{n(n+1)/2}$ with coordinates $\lambda_j^{(k)}$ ($1 \leq i \leq k \leq n$) satisfying the interlacing inequalities (2.7) for all k [GS83a]. This set, which we denote $\Delta_{\lambda^{(n+1)}}$, is the *unitary Gelfand–Zeitlin (GZ) polytope* associated to $\lambda^{(n+1)}$. The inequalities defining this polytope are typically represented in a triangular array, as illustrated in the following diagram for the case $n = 2$.

$$\begin{array}{ccccc} \lambda_1^{(3)} & & \lambda_2^{(3)} & & \lambda_3^{(3)} \\ & \searrow & & \searrow & \\ & \lambda_1^{(2)} & & \lambda_2^{(2)} & \\ & & \searrow & & \\ & & \lambda_1^{(1)} & & \end{array} \quad (2.8)$$

To every point in $\Delta_{\lambda^{(n+1)}}$, we associate a *unitary Gelfand–Zeitlin (GZ) pattern* which is a plane graph drawn as follows. Starting from the triangular array of inequalities, as in the example

above, replace the numbers $\lambda_j^{(k)}$ with vertices. Draw an edge between two nearest neighbour vertices if the associated numbers are equal. An example of a unitary GZ pattern is illustrated in Figure 4. *Row k* of a unitary GZ pattern is the full subgraph on the row of vertices corresponding to the numbers $\lambda_1^{(k)}, \dots, \lambda_k^{(k)}$. Note that the unitary GZ pattern of a point in $\Delta_{\lambda^{(n+1)}}$ only depends on the face of $\Delta_{\lambda^{(n+1)}}$ which contains the point in its relative interior.

Fix now a point $(\lambda^{(n)}, \dots, \lambda^{(1)}) \in \Delta_{\lambda^{(n+1)}}$. Then $\Psi^{-1}(\lambda^{(n)}, \dots, \lambda^{(1)})$ is nonempty and the subgroups $L_k \leq H_k \leq G_k$ defined in the previous section are determined (up to conjugacy) by the associated unitary GZ pattern as follows.

1. For $1 \leq k \leq n$, let ℓ_k be the number of connected components of row k of the GZ pattern, and let d_j be the number of vertices in the j^{th} connected component of row k of the GZ pattern (ordering the connected components from left to right). Then H_k is the block diagonal subgroup

$$H_k = \mathrm{U}(d_1) \oplus \cdots \oplus \mathrm{U}(d_{\ell_k}) \leq \mathrm{U}(k). \quad (2.9)$$

2. For $1 \leq j \leq \ell_k$, let $K_j = \mathrm{U}(d_j)$ if the number of vertices in row $k+1$ that are connected to the j^{th} connected component of row k is $\geq d_j$. Otherwise, let K_j be the block diagonal subgroup $[1] \oplus \mathrm{U}(d_j - 1) \leq \mathrm{U}(d_j)$. Then L_k is the block diagonal subgroup

$$L_k = K_1 \oplus \cdots \oplus K_{\ell_k} \leq H_k \quad (2.10)$$

The condition in item 2 can be phrased more conveniently by introducing some terminology. Consider the full subgraph on rows k and $k+1$ of the GZ pattern. A connected component of this subgraph is a Δ -shape if it contains more vertices from row k than $k+1$, a ∇ -shape if it contains more vertices from row $k+1$ than k , and a \square -shape if it contains the same number of vertices in row k as in row $k+1$. Thus, $K_j = [1] \oplus \mathrm{U}(d_j - 1)$ if the associated connected component is a Δ -shape and $K_j = \mathrm{U}(d_j)$ otherwise. This terminology of \square -shape/ ∇ -shape/ Δ -shape is equivalent to the N-block/W-block/M-block terminology used for ladder diagrams (which are equivalent to GZ patterns) of Cho–Kim–Oh [CKO20].

We briefly outline how to derive the descriptions of H_k and L_k above. The description of H_k follows immediately since H_k is the stabilizer of the diagonal matrix with diagonal entries $\lambda_1^{(k)}, \dots, \lambda_k^{(k)}$. The description of L_k follows by computing the stabilizer of a point ζ_k in the preimage of this diagonal matrix. This computation employs the characteristic polynomial of ζ_k , which is how the interlacing inequalities come into play in the description of L_k [CKO20, §5].

Example 2.11. We briefly illustrate these definitions with an example. Consider the unitary GZ pattern in Figure 4. Looking at rows 4 and 5, we see that $H_4 = \mathrm{U}(4)$ and $L_4 = [1] \oplus \mathrm{U}(3)$. Looking at rows 6 and 7, we see that

$$H_6 = \mathrm{U}(2) \oplus \mathrm{U}(2) \oplus \mathrm{U}(1) \oplus \mathrm{U}(1), \quad L_6 = ([1] \oplus \mathrm{U}(1)) \oplus \mathrm{U}(2) \oplus \mathrm{U}(1) \oplus \mathrm{U}(1).$$

Looking at the penultimate row 9, we see $H_9 \cong \mathrm{U}(2) \oplus \mathrm{U}(1)^{\oplus 2} \oplus \mathrm{U}(2) \oplus \mathrm{U}(1)^3$ whereas $L_9 \cong \mathrm{U}(2) \oplus \mathrm{U}(0)^2 \oplus \mathrm{U}(2) \oplus \mathrm{U}(0) \oplus \mathrm{U}(1) \oplus \mathrm{U}(0)$. We only look at row 10 in conjunction with row 9 to determine what the Δ -, ∇ -, and \square -shapes are; while H_{10} is defined, L_{10} is not. It does not make sense to refer to Δ -shapes, for example, in row 10, since there is no row 11.

2.3. The orthogonal case

This section describes orthogonal Gelfand–Zeitlin systems and their fibers as a special case of the setup in Section 2.1. Throughout this section, we write $[k]$ for $\lfloor k/2 \rfloor$, where $\lfloor \cdot \rfloor$ is the floor function.

For $k = 2, \dots, n+1$, let G_k be the group $\mathrm{SO}(k)$ of special orthogonal $k \times k$ matrices and let T_k be the standard maximal torus of G_k . The coadjoint representation of G_k on \mathfrak{g}_k^* can be identified linearly with action of G_k by conjugation on the space of $k \times k$ real skew-symmetric matrices. For k even, $\mathfrak{t}_{k,+}^*$ can be identified with the set of points $\lambda^{(k)} = (\lambda_1^{(k)}, \dots, \lambda_{[k]}^{(k)}) \in \mathbb{R}^{[k]}$ such that

$$\lambda_1^{(k)} \geq \lambda_2^{(k)} \geq \dots \geq \lambda_{[k]-1}^{(k)} \geq |\lambda_{[k]}^{(k)}| \quad (2.12)$$

and for k odd, $\mathfrak{t}_{k,+}^*$ can be identified with the set of points $\lambda^{(k)} \in \mathbb{R}^{[k]}$ such that

$$\lambda_1^{(k)} \geq \lambda_2^{(k)} \geq \dots \geq \lambda_{[k]}^{(k)} \geq 0. \quad (2.13)$$

We make these identification such that for k odd, $\mathcal{O}_{\lambda^{(k)}}$ is identified with the set of $k \times k$ skew-symmetric matrices with eigenvalues $\pm i\lambda_1^{(k)}, \dots, \pm i\lambda_{[k]}^{(k)}, 0$. For k even the special orthogonal conjugacy class of a skew-symmetric $k \times k$ matrix depends both on its eigenvalues and the sign of its Pfaffian. We make these identifications such that for k even, $\mathcal{O}_{\lambda^{(k)}}$ is identified with the set of $k \times k$ skew-symmetric matrices ζ with eigenvalues $\pm i\lambda_1^{(k)}, \dots, \pm i\lambda_{[k]}^{(k)}$ whose Pfaffian $\mathrm{Pf} \zeta$ satisfies $\lambda_{[k]}^{(k)} = \mathrm{sign}(\mathrm{Pf} \zeta) \cdot |\lambda_{[k]}^{(k)}|$. As in the unitary case, the choice of embeddings $\varphi_k: G_k \rightarrow G_{k+1}$ does not matter, but for the sake of concreteness, we set $\varphi_k(g) := g \oplus [1]$. With these choices, the map Ψ defined in (2.2) is a GZ system on any coadjoint orbit $\mathcal{O}_{\lambda^{(n+1)}}$ of $\mathrm{SO}(n+1)$ [GS83b].

The interlacing inequalities that characterize for which values of $\lambda^{(k)}$ and $\lambda^{(k+1)}$ the intersection $\mathcal{O}_{\lambda^{(k+1)}, \lambda^{(k)}}$ is non-empty depend on the parity of k . For k odd, they are

$$\begin{array}{ccccccccc} \lambda_1^{(k+1)} & & \lambda_2^{(k+1)} & & \lambda_3^{(k+1)} & & \lambda_{[k+1]-1}^{(k+1)} & & |\lambda_{[k+1]}^{(k+1)}| \\ & \searrow & & \searrow & & \searrow & & \searrow & \\ & \lambda_1^{(k)} & & \lambda_2^{(k)} & & \dots & & \lambda_{[k]}^{(k)} & \end{array} \quad (2.14)$$

whereas for k even, they are

$$\begin{array}{ccccccccc} \lambda_1^{(k+1)} & & \lambda_2^{(k+1)} & & \lambda_3^{(k+1)} & & \lambda_{[k+1]}^{(k+1)} & & \\ & \searrow & & \searrow & & \searrow & & \searrow & \\ & \lambda_1^{(k)} & & \lambda_2^{(k)} & & \dots & & |\lambda_{[k]}^{(k)}| & \end{array} \quad (2.15)$$

See Pabiniak [Pab12, App. B] for a proof. In both cases, the pattern of inequalities can be extended symmetrically by including 0 and the non-positive eigenvalues. The image of the GZ system on $\mathcal{O}_{\lambda^{(n+1)}}$ is the set of points in $\mathbb{R}^{\sum_{k=1}^n [k]}$ whose coordinates $\lambda_j^{(k)}$ for $1 \leq k \leq n$ and $1 \leq j \leq [k]$ satisfy the interlacing inequalities above. This set, which we denote $\Delta_{\lambda^{(n+1)}}$, is the *orthogonal Gelfand–Zeitlin (GZ) polytope* associated to $\lambda^{(n+1)}$. We may represent these inequalities in a triangular array, as illustrated in the following diagram for the case $n = 4$. One may omit the right side and the zero in the bottom row without loss of information, but we opt to keep these features because

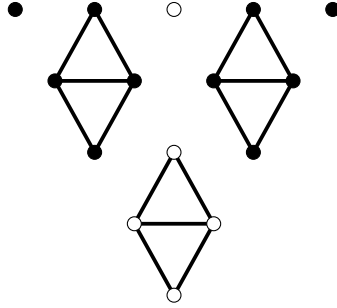


Figure 17: An orthogonal GZ pattern associated to a fiber of a GZ system on a coadjoint orbit of $\text{SO}(5)$.

they help simplify some descriptions later on.

$$\begin{array}{cccccccc}
 \lambda_1^{(5)} & & \lambda_2^{(5)} & & 0 & & -\lambda_2^{(5)} & & -\lambda_1^{(5)} \\
 \Downarrow & \nearrow & \Downarrow & \nearrow & \Downarrow & \nearrow & \Downarrow & \nearrow & \Downarrow \\
 & \lambda_1^{(4)} & & |\lambda_2^{(4)}| & & -|\lambda_2^{(4)}| & & -\lambda_1^{(4)} & \\
 & \Downarrow & \nearrow & \Downarrow & \nearrow & \Downarrow & \nearrow & \Downarrow & \\
 & & \lambda_1^{(3)} & & 0 & & -\lambda_1^{(3)} & & \\
 & & \Downarrow & \nearrow & \Downarrow & \nearrow & \Downarrow & \nearrow & \\
 & & & |\lambda_1^{(2)}| & & -|\lambda_1^{(2)}| & & & \\
 & & & \Downarrow & \nearrow & \Downarrow & \nearrow & & \\
 & & & & 0 & & & &
 \end{array} \tag{2.16}$$

Orthogonal Gelfand–Zeitlin (GZ) patterns are drawn in a similar manner as the unitary case. In order to simplify our description of the subgroups H_k and L_k that follow, we colour vertices corresponding to 0 white. This vertex colouring is purely for convenience of exposition; no information is lost by omitting it since the connected components intersecting the vertical midline must correspond to 0. All other vertices are black. For example, if in the case $n = 4$ illustrated above the values are $\lambda_1^{(5)} = 2$, $\lambda_2^{(5)} = \lambda_1^{(4)} = -\lambda_2^{(4)} = \lambda_1^{(3)} = 1$, and $\lambda_1^{(2)} = 0$, then the GZ pattern is given as in Figure 17. *Row k* of an orthogonal GZ pattern is defined as in the unitary case. The bottom vertex is necessarily white, since it corresponds to 0. The full subgraph on the black vertices to the left of the vertical midline is the *positive part* of the orthogonal GZ pattern. The full subgraph on the black vertices to the right of the vertical midline is the *negative part*. The negative part is a mirror reflection of the positive part. One may omit the negative part of the orthogonal GZ pattern without losing any information.

Fix a point $(\lambda^{(n)}, \dots, \lambda^{(2)}) \in \Delta_{\lambda^{(n+1)}}$. As in the unitary case, the subgroups $L_k \leq H_k \leq G_k$ are determined (up to conjugacy) by the associated orthogonal GZ pattern. The description is as follows.

1. For $2 \leq k \leq n$, let $2\ell_k$ be the number of connected components of row k which do not contain a white vertex. Let d_0 be the number of vertices in the connected component with white vertices, and for $1 \leq i \leq \ell_k$, let d_i be the number of vertices in the i^{th} connected component of row k as indexed from left to right.

Then the subgroup H_k is isomorphic to the product

$$\text{U}(d_1) \times \cdots \times \text{U}(d_{\ell_k}) \times \text{SO}(d_0) \tag{2.18}$$

where $\mathrm{SO}(1) \cong \mathrm{SO}(0) := \{1\}$. Note that d_0 must be congruent to k modulo 2. The equalities and strict inequalities occurring in (2.12) or (2.13) for the given value of $\lambda^{(k)}$ determine a subgraph of the Dynkin diagram of G_k , which in turn determines a Levi factor whose compact form is the desired embedding of the product group above as the subgroup H_k .³

2. For $1 \leq i \leq \ell_k$, let $K_i = \mathrm{U}(d_i)$ if the number of vertices in row $k+1$ that are connected to the i^{th} connected component of row k is $\geq d_i$ and otherwise let $K_i = [1] \oplus \mathrm{U}(d_i - 1) \leq \mathrm{U}(d_i)$. Let $K_0 = \mathrm{SO}(d_0)$ if the number of white vertices in row $k+1$ is $\geq d_0$, and otherwise, let $K_0 = \mathrm{SO}(d_0 - 1) \leq \mathrm{SO}(d_0)$, where $\mathrm{SO}(1) \cong \mathrm{SO}(0) = \mathrm{SO}(-1) := \{1\}$. Then L_k is the block diagonal subgroup

$$L_k = K_1 \times \cdots \times K_{\ell_k} \times K_0 \leq H_k. \quad (2.19)$$

As in the unitary case, one can use the language of \square -shape/ ∇ -shape/ \triangle -shape to state the condition in item 2 that determines the groups K_i . The description of the subgroups H_k and L_k is derived in a similar manner to that in the unitary case. We note that the description of the subgroups H_k and L_k given here diverges slightly from that of Cho and Kim, due to an error in their statement of their Lemma 6.5 [CK20]. This minor error does not affect their main results.

Example 2.20. Consider the orthogonal GZ pattern in Figure 17. Looking at rows 4 and 5 we see that $H_4 = \mathrm{U}(2) \times \mathrm{U}(2)$ and $L_4 = ([1] \oplus \mathrm{U}(1)) \times ([1] \oplus \mathrm{U}(1))$. Looking at rows 3 and 4 we see that $H_3 = L_3 = \mathrm{U}(1) \times \mathrm{U}(1)$. Looking at rows 2 and 3 we see that $H_2 = \mathrm{SO}(2)$ and L_2 is the trivial group.

3. The structure of Gelfand–Zeitlin fibers

We start by re-writing the towers of Cho–Kim–Oh introduced in the previous section, as balanced products (Theorem 3.2). A direct product decomposition of GZ fibers, which is new in the orthogonal case, follows immediately from this description (Corollary 3.3). We will use this direct product decomposition to analyze the cohomology of orthogonal GZ fibers in Section 5. In the discussion following Corollary 3.3, we show how each factor in the direct product decomposition can be simplified using the combinatorics of the GZ pattern. Our simplified description in terms of the GZ pattern is summarized in Theorem 3.8. We end the section with examples demonstrating how Theorem 3.8 can be applied. In particular, we recover Bouloc, Miranda, and Zung’s description of regular, elliptic, and (multi-)diamond fibers of unitary GZ systems as a special case of Theorem 3.8.

We begin with a general lemma. Suppose a group G acts on the right on a space X and on the left on a space Y . In this case, we define the *balanced product* $X \otimes_G Y$ to be the quotient $(X \times Y)/G$ under the diagonal action. The elements of $X \otimes_G Y$, which we denote $x \otimes y$, satisfy $xg \otimes y = x \otimes gy$.

³One must be careful in the case where k is even and $d_0 = 0$: the cases $\lambda_{[k]}^{(k)} > 0$ and $\lambda_{[k]}^{(k)} < 0$ correspond to two different subgraphs of the Dynkin diagram and hence to distinct embeddings of H_k as a subgroup of G_k . These two embeddings differ in how the factor $\mathrm{U}(\ell_k)$ is embedded (they are conjugate to one another by an element of $\mathrm{SO}(k+1)$ but not by an element of $\mathrm{SO}(k)$). This dichotomy is not reflected in the orthogonal GZ diagrams defined above and does not affect the rest of our analysis, so we will not further belabour it.

Lemma 3.1. *Let $\psi: G \rightarrow \tilde{G}$ be a map of topological groups and let $L \leq G$ and $\tilde{L} \leq \tilde{H} \leq \tilde{G}$ be closed subgroups such that $\psi(L) \leq \tilde{H}$. Suppose \tilde{L} acts continuously on a topological space X . Then the map*

$$\begin{aligned} \varkappa: G/L \times_{\tilde{G}/\tilde{H}} \tilde{G} \otimes_{\tilde{L}} X &\longrightarrow G \otimes_L \tilde{H} \otimes_{\tilde{L}} X, \\ (gL, \tilde{g} \otimes x) &\longmapsto g \otimes \varphi(g)^{-1} \tilde{g} \otimes x, \end{aligned}$$

is a well-defined homeomorphism. If the homomorphisms are of compact Lie groups and X is a smooth manifold with smooth \tilde{L} -action, then \varkappa is a diffeomorphism.

Proof. Since the fiber product $G \times_{\tilde{G}/\tilde{H}} \tilde{G}$ is the set of pairs $(g, \tilde{g}) \in G \times \tilde{G}$ such that $\varphi(g)^{-1} \tilde{g}$ lies in \tilde{H} , it is easy to see the assignments $(g, \tilde{g}) \mapsto (g, \varphi(g)^{-1} \tilde{g})$ and $(g, \tilde{h}) \mapsto (g, \varphi(g) \tilde{h})$ define a continuous map $G \times_{\tilde{G}/\tilde{H}} \tilde{G} \rightarrow G \times \tilde{H}$ and its continuous inverse. One checks using coset representatives that these maps descend to well-defined maps $\kappa: G/L \times_{\tilde{G}/\tilde{H}} \tilde{G} \rightarrow G \otimes_L \tilde{H}$ and κ^{-1} , necessarily homeomorphisms, and then that $\kappa \times \text{id}_X$ and $\kappa^{-1} \times \text{id}_X$ descend to a well-defined \varkappa and its well-defined inverse \varkappa^{-1} . Under the smoothness hypotheses, the original homeomorphism and its inverse are smooth, and as all the actions in question are free and proper, so the orbit spaces are again smooth manifolds and the quotient maps are smooth submersions, meaning \varkappa and \varkappa^{-1} are smooth as well. \square

The following result applies equally to both unitary and orthogonal GZ systems.

Theorem 3.2. *Let $G_k = \text{U}(k)$ for all $1 \leq k \leq n+1$ or let $G_k = \text{SO}(k)$ for all $1 \leq k \leq n+1$. In either case, let Ψ be the GZ system on a coadjoint orbit \mathcal{O}_λ of G_{n+1} , let p be a point in the associated GZ polytope Δ_λ , and let $L_k \leq H_k \leq G_k$ be defined via the GZ pattern of p (as in Section 2.2 in the unitary case, and as in Section 2.3 in the orthogonal case). Then there is a diffeomorphism*

$$\Psi^{-1}(p) \cong H_a \otimes_{L_a} H_{a+1} \otimes_{L_{a+1}} \cdots \otimes_{L_{n-1}} H_n/L_n$$

where the balanced products with respect to the groups L_k are taken with respect to the natural inclusion of L_k into H_k and the embedding of L_k into H_{k+1} via the homomorphism $A\varphi_k A^{-1}: G_k \rightarrow G_{k+1}$, where $A \in G_{k+1}$ satisfies $\text{Ad}_A^* \zeta_k = \lambda^{(k+1)}$.

Proof. Consider the diagram of Figure 3. At each level, fix the compositions (2.5) to be $\iota_{A,A}$, as defined in (2.5), which as noted at the end of Section 2.1 are induced by the homomorphisms $A\varphi_k A^{-1}: G_k \rightarrow G_{k+1}$ sending L_k into H_{k+1} .

We will more generally prove a diffeomorphism

$$F_j^k \cong G_j \otimes_{L_j} H_{j+1} \otimes_{L_{j+1}} \cdots \otimes_{L_{k-2}} H_{k-1} \otimes_{L_{k-1}} *, \quad (a \leq j < k \leq n+1).$$

The result follows since $G_a = H_a$ and $F_a^{n+1} \cong \Psi^{-1}(p)$, as explained in Section 2.1.

The claim is proved separately for each k by decreasing (i.e., leftward) induction on the horizontal index j . For the base case when $j = k-1$, the expression simplifies to $F_{k-1}^k \cong G_{k-1}/L_{k-1}$. For the induction step, assume the diffeomorphism for j and consider the rectangle

$$\begin{array}{ccc} F_{j-1}^k & \twoheadrightarrow & F_j^k \\ \downarrow & & \downarrow \\ F_{j-1}^j & \twoheadrightarrow & F_j^j \end{array}$$

comprising vertically stacked boxes in (3). We have $F_{j-1}^j = G_{j-1}/L_{j-1}$ and $F_j^j = G_j/H_j$, and the inductive assumption gives an expression $G_j \otimes_{L_j} X$ for F_j^k . An application of Lemma 3.1 to this X and $(G, L) = (G_{j-1}, L_{j-1})$ and $(\tilde{G}, \tilde{H}, \tilde{L}) = (G_j, H_j, L_j)$ then completes the induction. \square

Corollary 3.3. *Every Gelfand–Zeitlin fiber corresponding to a unitary or orthogonal Gelfand–Zeitlin pattern is diffeomorphic to a direct product of factors indexed by the connected components of the Gelfand–Zeitlin pattern. Pairs of connected components in the positive and negative part of an orthogonal Gelfand–Zeitlin pattern contribute a single connected component.*

Proof. The groups L_k and H_k decompose into direct products of factors which correspond to connected components of the k th row of the GZ pattern, and the inclusion $L_k \rightarrow H_k$ is a direct product of inclusions of these factors. Again, fix $A \in G_{k+1}$ such that $\text{Ad}_A^* \zeta_k = \lambda^{(k+1)}$. One can show that the maps $A\varphi_k A^{-1}: L_k \rightarrow H_{k+1}$ decompose as direct products with the property that each factor of L_k is mapped to the factor of H_{k+1} corresponding to the same connected component of the GZ pattern. In general, given a tuple of diagrams $M_j \leftarrow K_j \rightarrow N_j$ of groups one has $\prod M_j \otimes_{\prod K_j} \prod N_j \cong \prod (M_j \otimes_{K_j} N_j)$. Thus, the desired direct product splitting of the GZ fibers follows by Theorem 3.2. \square

We now explain how the preceding description of arbitrary GZ fibers can be simplified; afterwards we will give several concrete examples. By Corollary 3.3, it suffices to describe the direct product factor corresponding to an arbitrary connected component of a GZ pattern. Thus, suppose for the remainder of this discussion that we are given a connected component of a GZ pattern (unitary or orthogonal) beginning in row k_b and ending in row k_t . For any integer $k \in [k_b, k_t]$, write $w(k)$ for the *width* of row k of the component, i.e., the number of vertices in the component in this row. The width $w(k_b)$ of the bottom row in the connected component is always 1, and $w(k_t)$ is also 1 unless $k_t = n + 1$, meaning the component ends in the top row of the GZ pattern. As this case requires a slightly different analysis, for now we assume that $k_t \leq n$.

A direct factor corresponding to the given connected component is of the form

$$J_{k_b} \otimes_{K_{k_b}} J_{k_b+1} \otimes_{K_{k_b+1}} \cdots \otimes_{K_{k_t-2}} J_{k_t-1} \otimes_{K_{k_t-1}} J_{k_t} \quad (3.4)$$

where the factors $K_k \leq J_k$ for $k_b \leq k \leq k_t$ are the factors of L_k and H_k (respectively) described by (2.9) and (2.10) in the unitary case and (2.18) and (2.19) in the orthogonal case. Note that K_{k_t} is trivial since $k_t \leq n$. For a black component (one of a pair, in the orthogonal case), we have $J_k \cong U(w(k))$, and for a white component, we have $J_k \cong \text{SO}(w(k))$.

We may usually simplify the expression (3.4) as follows. For each integer $k \in [k_b, k_t - 1]$, the expression contains a factor $J_k \otimes_{K_k} J_{k+1}$ determined by the pair of consecutive rows $k, k + 1$. When these rows form an \triangle -shape or a \square -shape, then $K_k = J_{k+1}$ so we have the simplification $J_k \otimes_{K_k} J_{k+1} \cong J_k$, whereas if they form a ∇ -shape, then $K_k = J_k$, so we have $J_k \otimes_{K_k} J_{k+1} \cong J_{k+1}$. Iterating the procedure, one can always simplify (3.4) into the following equivalent forms. First, if each row is of width 1, then the expression collapses to one factor, $U(1)$ for a black component or $\text{SO}(1) = *$ for a white component. Otherwise, take a subsequence

$$\tilde{\ell}_1 \leq \ell_1 \leq \tilde{\ell}_2 \leq \ell_2 \leq \cdots \leq \tilde{\ell}_{r-1} \leq \ell_{r-1} \leq \tilde{\ell}_r,$$

of $[k_b + 1, k_t - 1]$ such that $M_i = w(\tilde{\ell}_i)$ and $m_i = w(\ell_i)$ are, respectively, sequences of local maximum and minimum values of the function w on the interval $[k_b, k_t]$. The sequence M_i begins

with the first local maximum and terminates with the last local maximum. Although the values $w(k_b) = w(k_t) = 1$ are necessarily local minima, we ignore them since they correspond to factors which cancel. The sequence m_i begins with the second local minimum and ends with the penultimate local minimum of the function w on the interval $[k_b + 1, k_t - 1]$. Then the expression (3.4) simplifies to $J_{\tilde{\ell}_1} \otimes_{K_{\ell_1}} J_{\tilde{\ell}_2} \otimes_{K_{\ell_2}} \cdots \otimes_{K_{\ell_{r-1}}} J_{\tilde{\ell}_r}$, which is

$$\mathrm{U}(M_1) \otimes_{\mathrm{U}(m_1)} \cdots \otimes_{\mathrm{U}(m_{r-1})} \mathrm{U}(M_r) \quad \text{or} \quad \mathrm{SO}(M_1) \otimes_{\mathrm{SO}(m_1)} \cdots \otimes_{\mathrm{SO}(m_{r-1})} \mathrm{SO}(M_r) \quad (3.5)$$

depending on whether the component is black or white. In the case of a white component, this expression corresponds to a decomposition of the component into maximal hexagons and pentagons.

Now we treat the special case $k_t = n + 1$. In this case, there is no group J_{n+1} . A direct product factor corresponding to the given connected component has the form

$$J_{k_b} \otimes_{K_{k_b}} J_{k_b+1} \otimes_{K_{k_b+1}} \cdots \otimes_{K_{n-1}} J_n/K_n. \quad (3.6)$$

This expression can be simplified by a similar analysis to that in the preceding paragraph. In the degenerate case where each row is of width 1, the expression collapses to $\mathrm{U}(1)/\mathrm{U}(1)$ or $\mathrm{SO}(1)/\mathrm{SO}(1)$, which is a point either way. Otherwise, restrict the function w to the subset $[k_b, k_t - 1]$ and let $\tilde{\ell}_i, \ell_i$ denote the sequence of arguments which achieve local maxima and minima for the function w on this subset (as before). Then, similarly to before, the expression (3.6) simplifies to $J_{\tilde{\ell}_1} \otimes_{K_{\ell_1}} J_{\tilde{\ell}_2} \otimes_{K_{\ell_2}} \cdots \otimes_{K_{\ell_{r-1}}} J_{\tilde{\ell}_r}/K_n$. More explicitly, depending on whether it is a black or white component respectively, this equals

$$\mathrm{U}(M_1) \otimes_{\mathrm{U}(m_1)} \cdots \otimes_{\mathrm{U}(m_{r-1})} \mathrm{U}(M_r)/K_n \quad \text{or} \quad \mathrm{SO}(M_1) \otimes_{\mathrm{SO}(m_1)} \cdots \otimes_{\mathrm{SO}(m_{r-1})} \mathrm{SO}(M_r)/K_n \quad (3.7)$$

where $M_i = w(\tilde{\ell}_i)$ and $m_i = w(\ell_i)$ as before. The group K_n is determined by the shape that occurs in the connected component between the top two rows (see examples below). It will be useful later that this expression gives a different iterated fiber bundle construction for F_a^{n+1} with base $J_{\tilde{\ell}_1}/K_{\ell_1}$ and fibers $J_{\tilde{\ell}_i}/K_{\ell_i}$ and either $J_{\tilde{\ell}_r}$ or $J_{\tilde{\ell}_r}/K_n$.

These direct factors can also be realized as biquotients. Recall that if A and B are closed subgroups of a Lie group G such that the action $(a, b) \cdot g = agb^{-1}$ of $A \times B$ on G is free, then the orbit space is called a *biquotient* and denoted $A \backslash G / B$.

Theorem 3.8 (Biquotient description). *Every direct product factor of a GZ fiber can be written as a biquotient $A \backslash G / B$ as follows. Let $\tilde{\ell}_i$ and ℓ_i be the indices of rows with local maximum and minimum widths, respectively, as above, excluding the first and last rows.*

$$G = J_{\tilde{\ell}_1} \times J_{\tilde{\ell}_2} \times \cdots \times J_{\tilde{\ell}_r} \quad (3.9)$$

and the subgroups A and B have the forms

$$\begin{aligned} A &= \{(1, j_2, j_2, j_4, j_4, \dots) \in G : j_{2i} \in K_{2\ell_i}\}, \\ B &= \{(j_1, j_1, j_3, j_3, \dots) \in G : j_{2i-1} \in K_{2\ell_{i-1}}\}. \end{aligned} \quad (3.10)$$

If the component ends in the top row $n + 1$, then one of the subgroups A or B will additionally include the factor K_n in the last coordinate.

Proof. This follows immediately from the discussion above, the map from the biquotient to the balanced product explicitly being given by $A(g_1, g_2, g_3, g_4, \dots)B \mapsto g_1 \otimes g_2^{-1} \otimes g_3 \otimes g_4^{-1} \otimes \dots$ in the case $k_t \leq n$ and similarly when $k_t = n + 1$. \square

We now illustrate our general description of the fibers with several examples. The first few examples demonstrate how the description above recovers previously known facts about unitary GZ fibers.

Example 3.11 (Torus fibers in unitary GZ systems). As noted above, a connected component of a unitary GZ pattern that has maximum width equal to 1 and ends below the top row contributes a factor of $U(1)$, i.e., a circle. A connected component ending in the top row and with $w(k)$ nondecreasing contributes $U(w(n))/U(w(n))$, i.e., a point. In particular, a unitary GZ fiber is a torus if and only if every connected component all the connected components of the associated GZ pattern have one of these forms. In this case, the dimension of the torus is the number of connected components not connected to the top row. This recovers the description of “regular fibers” and “elliptic non-degenerate singular fibers” given by Bouloc *et al.* [BouMZ18, §5].

Example 3.12 (Diamonds in unitary GZ patterns). Suppose that a connected component of a unitary GZ pattern is such that the sequence of local minimum and maximum widths, omitting first and last rows, contains a single entry (necessarily a local maximum, with $w \geq 2$). If the component ends before the top row, the corresponding direct factor is $U(w)$. If it ends in the top row, the corresponding factor is $U(w)/U(1) \cong SU(w)$. In the special case where the sequence of widths strictly increases to w and strictly decreases afterward, this recovers the existing description of “diamond singularities” [BouMZ18, §5].

In the orthogonal case, the black connected components of orthogonal GZ patterns are treated as in the unitary case, with the only difference being that each mirror pair of positive and negative connected components contributes a single factor to the direct product.

Example 3.13 (Torus fibers in orthogonal GZ systems). A white connected component consisting of an isolated vertex contributes a point. A white diamond of width 2 (i.e., a white connected component consisting of three rows with widths 1, 2, 1) contributes $SO(2)/SO(1)$, i.e., a circle. A white connected component ending in the top row and with $w(k)$ nondecreasing contributes a point. An orthogonal GZ fiber is a torus if and only if all the white components have one of these forms and all the black components have one of the forms from Example 3.11.

Example 3.14 (Diamonds in orthogonal GZ patterns). Suppose a white connected component of an orthogonal GZ pattern is a diamond of width $w \geq 2$, i.e., the sequence of local minimum and maximum widths increases to w and then decreases to 1. Then the corresponding direct product factor is $SO(w)$.

Example 3.15. Consider the orthogonal GZ pattern in Figure 17. The black diamond in the positive part contributes a factor of $U(2)/U(1) \cong SU(2)$ and the white diamond of width 2 contributes a factor of $SO(2)$. Thus, the GZ fiber is diffeomorphic to $SU(2) \times SO(2)$.

It will be important to our later analysis that all connected real and complex Stiefel manifolds (i.e., all but $O(n)$) can be realized as GZ fibers

Example 3.16 (Stiefel manifolds). Suppose a connected component of a GZ pattern contains vertices in the top row and the sequence of widths weakly increases from 1 to $w = w(\ell)$ and thereafter weakly decreases to $v = k(n + 1)$. For instance the component could be a pentagon,

as illustrated in Example 5.5 (this is the only possibility if the component is white). The corresponding direct factor is the complex Stiefel manifold $V_{w-v}(\mathbb{C}^w) \cong U(w)/U(v)$ if the component is black, and the real Stiefel manifold $V_{w-v}(\mathbb{R}^w) \cong O(w)/O(v) \cong SO(w)/SO(v)$ if it is white. Since we saw the unitary groups $V_w(\mathbb{C}^w) \cong U(w)$ realized as GZ fibers in Example 3.14, every complex and real Stiefel manifold except for the disconnected $V_w(\mathbb{R}^w) \cong O(w)$ occurs as a GZ fiber.

The splitting in Corollary 3.3 is not the end of the story on product decompositions of GZ fibers. For one thing, since $SO(1) = 1$, a “pinch” row of width 1 in a white component corresponds to a direct product splitting $X \otimes_{SO(1)} Y \cong X \times Y$.

For another, if $M_1 \leq M_2$ in the notation of (3.5) the map

$$\begin{aligned} U(M_1) \otimes_{U(m_1)} U(M_2) \otimes_{U(m_2)} Z &\longrightarrow \left(U(M_1)/U(m_1) \right) \times U(M_2) \otimes_{U(m_2)} Z, \\ g \otimes h \otimes z &\longmapsto (gU(m_1), gh \otimes z) \end{aligned}$$

is a diffeomorphism with inverse $(gU(m_1), h' \otimes z) \longmapsto g \otimes g^{-1}h' \otimes z$, and similarly if the groups are special orthogonal. Thus one can break off direct Stiefel manifold factors from the left until one encounters a local maximum width $M_p > M_{p+1}$. In the case the pattern component terminates before the top row yielding an expression of the form (3.6) and $M_r < M_{r-1}$, one can also peel Stiefel factors from the right-hand side of (3.6). Although not generally applicable, this process can be used in some sense three quarters of the time to split off at least one Stiefel direct factor from a pattern component ending below the top row and half the time for a component ending in the top row. The simplest examples for which this is not possible are

$$U(3) \otimes_{U(1)} U(2)/U(1) \quad \text{and} \quad U(3) \otimes_{U(1)} U(2) \otimes_{U(1)} U(3).$$

Remark 3.17. One might hope that even when a GZ fiber is not a product of Stiefel manifolds, its cohomology might still be isomorphic to that of the product. In Theorem 5.11, we will see that this is true of its cohomology groups, but it is not generally true of the cohomology ring, as will show in Example 5.19.

The following example demonstrates how our description can be applied to unitary GZ fibers in more complicated situations. To our knowledge, the diffeomorphism types of GZ fibers associated to more complicated GZ patterns like the one in this example have not been given a simple description elsewhere in the literature.

Example 3.18. Consider the unitary GZ pattern in Figure 4. The double diamond on the left contributes $U(2) \otimes_{U(1)} U(2) \cong S^3 \times U(2) \cong (S^3)^2 \times S^1$, and the long connected component on the right contributes $U(2)/U(1) \cong S^3$; cf. Example 3.12.

Finally, the largest component contributes $U(4) \otimes_{U(2)} U(3)/U(2) \cong U(2) \setminus (U(4) \times U(3))/U(2)$. The factors associated to the remaining connected components are $U(1)$, as described as in Example 3.11. All told, the associated GZ fiber is diffeomorphic to

$$(S^1)^7 \times (S^3)^3 \times U(2) \setminus (U(4) \times U(3))/U(2).$$

Remark 3.19. We have found what seems to be another instance of the balanced product construction in work of Kajii, Kuroki, Lee, and Suh [KaKLS20, Defs. 3.1, 3.5]. They describe *generalized Bott towers* as iterated bundles with generalized flag manifolds K_i/Z_i as fibers and produce, using rather different methods from ours, an alternative description of these spaces as balanced

products. The total spaces of generalized Bott towers, although they also admit descriptions as balanced products, are different from GZ fibers, as their cohomology is concentrated in even degrees while, as we will show below, that of a unitary GZ fiber is generated in odd degrees.

4. Cohomology of unitary Gelfand–Zeitlin fibers

In this section we compute the cohomology of the fibers of Gelfand–Zeitlin systems on unitary coadjoint orbits. Our result is summarized in the following theorem.

Theorem 4.1. *The integer cohomology ring of a unitary GZ fiber is isomorphic to the exterior algebra*

$$\Lambda[z_{2d-1,i}], \quad |z_{2d-1,i}| = 2d - 1.$$

where the generators $z_{2d-1,i}$ enumerate all Δ -shapes in the associated Gelfand–Zeitlin pattern with width d , i.e., d vertices on the long edge.

We demonstrate this result with an example before proceeding to the proof.

Example 4.2. Enumerating Δ -shapes in the GZ pattern in Figure 4, we see that the integral cohomology ring of the associated GZ fiber is

$$\Lambda[z_{1,1}, z_{1,2}, z_{1,3}, z_{1,4}, z_{1,5}, z_{1,6}, z_{1,7}, z_{3,1}, z_{5,1}, z_{5,2}, z_{7,1}], \quad |z_{m,j}| = m.$$

Note that isolated vertices in the top row of the GZ pattern are not Δ -shapes of width 1.

By the general argument in Section 2.1, it suffices to compute the cohomology of the space F_1^{n+1} in the diagram of Figure 3 (with $a = 1$), where the maps $F_k^{k+1} \rightarrow F_k^k$ are the bundle projections of (2.4) and the maps $F_k^{k+1} \rightarrow F_{k+1}^{k+1}$ are the embeddings $\iota_{A,A}$ defined in (2.5). The groups $L_k \leq H_k \leq U(k)$ ($1 \leq k \leq n$) are defined as in Section 2.2 from the unitary Gelfand–Zeitlin pattern of the given point. For the remainder of this section, we write $\iota := \iota_{A,A}$, $F^k := F_1^k$, and $G_k = U(k)$. All cohomology will implicitly be taken with \mathbb{Z} coefficients.

Lemma 4.3. *The Serre spectral sequence of each bundle $F^{k+1} \rightarrow F^k$ collapses at E_2 .*

Proof. Let $\chi_k: U(k)/H_k \rightarrow BH_k$ be a classifying map for the principal H_k -bundle $U(k) \rightarrow U(k)/H_k$, and write $j_k: F^k \rightarrow F_k^k = U(k)/H_k$ for the composition of horizontal maps from F^k to F_k^k in the diagram of Figure 3. We will first prove by induction on k that $\chi_k \circ j_k$ induces the zero map in reduced cohomology. For $k = 1$, this is trivial since F^1 is a point. For the induction step, factor j_{k+1} as the composite of $\tilde{j}_k: F^{k+1} \rightarrow F_k^{k+1} = U(k)/L_k$ and the embedding $\iota: U(k)/L_k \rightarrow U(k+1)/H_{k+1}$. Let $\tilde{\chi}_k: U(k)/L_k \rightarrow BL_k$ be a classifying map for the principal L_k -bundle $U(k) \rightarrow U(k)/L_k$. If we model BL_k as EH_k/L_k , then we have maps of H_k/L_k -bundles as in the left diagram of (4.4) below. The square diagram on the right also commutes up to homotopy.

$$\begin{array}{ccccc}
F^{k+1} & \xrightarrow{\tilde{j}_k} & G_k/L_k & \xrightarrow{\tilde{\chi}_k} & BL_k \\
\downarrow & & \downarrow & & \downarrow \\
F^k & \xrightarrow{j_k} & G_k/H_k & \xrightarrow{\chi_k} & BH_k \\
\end{array}
\qquad
\begin{array}{ccc}
G_{k+1}/H_{k+1} & \xrightarrow{\chi_{k+1}} & BH_{k+1} \\
\uparrow \iota & & \uparrow \\
G_k/L_k & \xrightarrow{\tilde{\chi}_k} & BL_k
\end{array}
\tag{4.4}$$

These combine to yield the following commutative diagram in reduced cohomology.

$$\begin{array}{ccccc}
& & \tilde{H}^*(G_{k+1}/H_{k+1}) & \xleftarrow{\chi_{k+1}^*} & \tilde{H}^*(BH_{k+1}) \\
& \nearrow j_{k+1}^* & \downarrow i^* & & \downarrow \\
\tilde{H}^*(F^{k+1}) & \xleftarrow{\tilde{j}_k^*} & \tilde{H}^*(G_k/L_k) & \xleftarrow{\tilde{\chi}_k^*} & \tilde{H}^*(BL_k) \\
\uparrow & & \uparrow & & \uparrow \\
\tilde{H}^*(F^k) & \xleftarrow{j_k^*} & \tilde{H}^*(G_k/H_k) & \xleftarrow{\chi_k^*} & \tilde{H}^*(BH_k)
\end{array}$$

Since $H^*BU(m+1) \rightarrow H^*BU(m)$ is a surjection for all m , the map $H^*(BH_k) \rightarrow H^*(BL_k)$ is a surjection. By the inductive assumption, the bottom map $j_k^* \circ \chi_k^*$ is trivial, so it follows $\tilde{j}_k^* \circ \tilde{\chi}_k^*$ is trivial and hence $\tilde{j}_{k+1}^* \circ \chi_{k+1}^*$ is too, concluding the induction.

Now we can use the fact $\chi_k \circ j_k$ induces the zero map in reduced cohomology to see the spectral sequence of $F^{k+1} \rightarrow F^k$ collapses at E_2 . The maps of H_k/L_k -bundles on the left in (4.4) induce maps of Serre spectral sequences for each k . Every exterior generator z of the cohomology $H^*(H_k/L_k)$ of the fiber transgresses in the spectral sequence of $BL_k \rightarrow BH_k$ by comparison with the spectral sequences of the factors $BU(m) \xrightarrow{=} BU(m)$ and $BU(m) \rightarrow BU(m+1)$, say to τz . From the map of spectral sequences, we see z transgresses in the spectral sequence of $F^{k+1} \rightarrow F^k$ to the image of τz under the maps induced by $\chi_k \circ j_k$. But we have seen $(\chi_k \circ j_k)^* = 0$, so the spectral sequence of $F^{k+1} \rightarrow F^k$ collapses at E_2 . \square

The theorem follows easily.

Proof of Theorem 4.1. The proof has two parts. First, we prove by induction on k that

$$H^*(F^k) \cong \bigotimes_{\ell=1}^{k-1} H^*(H_\ell/L_\ell)$$

as graded rings. For $k = 1$ the claim is evident because the product is empty and F^1 is a point. For the induction step, note that by Lemma 4.3, the Serre spectral sequence of $F^{k+1} \rightarrow F^k$ collapses at E_2 so the associated graded algebra of $H^*(F^k)$ is $E_\infty = E_2 \cong H^*(F^k) \otimes H^*(H_k/L_k)$. By the inductive hypothesis, the underlying group is free abelian, so there is no additive extension problem, and particularly $H^*(F^{k+1})$ contains no 2-torsion. The lifts of a set of exterior generators for $H^*(H_k/L_k)$ along the fiber restriction $H^*(F^{k+1}) \rightarrow H^*(H_k/L_k)$ thus again square to zero and hence generate an exterior subalgebra Λ of $H^*(F^{k+1})$ isomorphic to $H^*(H_k/L_k)$. A basis of Λ also forms a basis for $H^*(F^{k+1})$ as an $H^*(F^k)$ -module, by the collapse and absence of an additive extension problem, so $H^*(F^{k+1})$ is the tensor product of Λ and $H^*(F^k)$, concluding the induction.

All that remains is to explicitly describe the factors $H^*(H_\ell/L_\ell)$ in this tensor product. It follows from the description of L_ℓ and H_ℓ given in Section 2.2 that H_ℓ/L_ℓ is a product of spheres of odd dimension. This product has a factor S^{2d-1} corresponding to each Δ -shape of width d that appears in rows k and $k+1$ of the GZ pattern. The theorem follows. \square

Remark 4.5. Cho–Kim–Oh [CKO20, Prop. 6.13] observe that a unitary GZ fiber splits as the direct product of a torus T and a space Y with $\pi_1(Y) = 0 = \pi_2(Y)$. That $\pi_2(F) = 0$ follows from an induction on the long exact sequence of the homotopy fibration, and to find T they use the torus action associated to the moment map. One can also deduce the splitting using just Lemma 4.3. Each H_k/L_k splits as the product of a torus $T_k \leq H_k$ and a product Y_k of spheres of dimension ≥ 3 , so we have a fiber bundle $Y_k \rightarrow E^k \rightarrow F^k$ and a principal bundle $T_k \rightarrow F^{k+1} \rightarrow E^k$. The latter bundle is trivial because the collapse implies the Euler classes $H^2(E^k)$ classifying the circle subbundles is trivial. It follows from our description that $\dim T$ is the number of Δ -shapes of width 1.

Knowing the cohomological structure makes a homological description available which, although it in a certain sense contains the same information, is in another sense more natural. The group structure on a Lie group G induces a map $H_*(G \times G; k) \rightarrow H_*(G; k)$ for any choice of coefficient ring k , and if this ring is a principal ideal domain chosen so that $H_*(G; k)$ is a free k -module, then using the Künneth theorem to make the identification $H_*(G; k) \otimes_k H_*(G; k) \cong H_*(G \times G; k)$, one has a composite $H_*(G; k) \otimes_k H_*(G; k) \rightarrow H_*(G; k)$ making $H_*(G; k)$ a graded ring (indeed, a Hopf algebra) called the *Pontrjagin ring*. This is the case for $k = \mathbb{Z}$ if $G = \mathrm{U}(n)$, and the resulting ring is an exterior algebra $\Lambda[u_1, u_3, \dots, u_{2n-1}]$ on generators $u_{2j-1} \in H_{2j-1}\mathrm{U}(n)$ dual to the cohomological exterior generators z_{2j+1} . When $m < n$, the map $H_*\mathrm{U}(m) \rightarrow H_*\mathrm{U}(n)$ induced by the standard subgroup inclusion is an injection taking u_{2j-1} to u_{2j-1} and the map $H_*\mathrm{U}(n) \rightarrow H_*(\mathrm{U}(n)/\mathrm{U}(m))$ is a quotient map annihilating the ideal generated by the u_{2j-1} with $j \in [1, m]$. We may suggestively write this as $H_*(\mathrm{U}(n)/\mathrm{U}(m)) \cong H_*\mathrm{U}(n) \otimes_{H_*\mathrm{U}(m)} \mathbb{Z}$, where \mathbb{Z} is a module over $H_*\mathrm{U}(m)$ via the augmentation induced by the map $\mathrm{U}(m) \rightarrow *$.⁴

Consider the quotient map

$$\pi : \mathrm{U}(4) \times \mathrm{U}(3) \rightarrow \mathrm{U}(4) \otimes_{\mathrm{U}(2)} \mathrm{U}(3)/\mathrm{U}(1) = X.$$

If we view π as the projection in a fiber bundle with fiber $\mathrm{U}(2) \times \mathrm{U}(1)$, then by computing ranks, we see its Serre spectral sequence collapses, so π induces an injection in cohomology and hence a surjection π_* in homology. To identify its image, note that two maps $\mathrm{U}(4) \times \mathrm{U}(2) \times \mathrm{U}(3) \rightarrow \mathrm{U}(4) \times \mathrm{U}(3)$ observe by $(g, h, g') \mapsto (gh, g')$ and $(g, h, g') \mapsto (g, hg')$ become the same map $(g, h, g') \mapsto gh \otimes g' = g \otimes hg'$ on postcomposing π . It follows that one has $\pi_*(\gamma\eta \otimes \gamma') = \pi_*(\gamma \otimes \eta\gamma')$ in $H_*(X)$ for any $(\gamma, \eta, \gamma') \in H_*\mathrm{U}(4) \times H_*\mathrm{U}(2) \times H_*\mathrm{U}(3)$, so that π_* factors through the quotient $Q = H_*\mathrm{U}(4) \otimes_{H_*\mathrm{U}(2)} H_*\mathrm{U}(3) \otimes_{H_*\mathrm{U}(1)} \mathbb{Z}$. But counting Δ -shapes in a GZ pattern component corresponding to X , we know its cohomology has rank $2^{4-2} \cdot 2^{3-1} = 16$, as does Q , so Q itself is the image of π_* .

The same reasoning holds for arbitrarily many factors.

Proposition 4.6. *Let a space X be given as on the left in (3.5) or (3.7) be given, writing $\mathrm{U}(q)$ for the trivial group $\mathrm{U}(0) = 1$ in the former case and for K_n in the latter. Then the quotient map*

$$\pi : \prod_{p=1}^r \mathrm{U}(M_p) \rightarrow \mathrm{U}(M_1) \otimes_{\mathrm{U}(m_1)} \cdots \otimes_{\mathrm{U}(m_{r-1})} \mathrm{U}(M_r)/\mathrm{U}(q) = X$$

induces a surjection in homology and an identification

$$H_*(X) \cong H_*\mathrm{U}(M_1) \otimes_{H_*\mathrm{U}(m_1)} \cdots \otimes_{H_*\mathrm{U}(m_{r-1})} H_*\mathrm{U}(M_r) \otimes_{H_*\mathrm{U}(q)} \mathbb{Z}.$$

⁴ One way to see this is to dualize from cohomology, and another is to emulate the equalization argument about to be presented.

Similar reasoning allows us to compute π_3 of a unitary GZ fiber.

Proposition 4.7. *The third homotopy group $\pi_3(F)$ of a unitary Gelfand–Zeitlin fiber F is free abelian. Its rank is the number of components of the graph obtained from the associated Gelfand–Zeitlin pattern by deleting all rows of width 1 from each component, then deleting any components still meeting the top row.*

Proof. Since π_3 distributes over direct products, it is enough to consider a factor X as described in Proposition 4.6 as the base space of a principal bundle with projection π and fiber $\prod U(m_p) \times U(q)$. Since π_2 of a Lie group is 0, the long exact homotopy sequence shows $\pi_3(X)$ is the cokernel of the map induced by the fiber inclusion. Thus

$$\pi_3(X) \cong \pi_3 U(M_1) \otimes_{\pi_3 U(m_1)} \cdots \otimes_{\pi_3 U(m_{r-1})} \pi_3 U(M_r) \otimes_{\pi_3 U(q)} 0.$$

Recalling that $\pi_3 U(1) = 0$ and for $n \geq m \geq 2$ the map $\pi_3 U(m) \rightarrow \pi_3 U(n) \cong \mathbb{Z}$ is an isomorphism, this tensor product breaks into a direct product for each p such that $m_p = 1$. If $q \geq 2$, then the last direct factor is 0, whereas otherwise it, like all the other direct factors, is of the form $\mathbb{Z} \otimes_{\mathbb{Z}} \cdots \otimes_{\mathbb{Z}} \mathbb{Z} \cong \mathbb{Z}$. \square

5. Cohomology of orthogonal Gelfand–Zeitlin fibers

As one might be led to expect from the more complicated descriptions of H_k and L_k in the orthogonal case, the computation of the cohomology of the Gelfand–Zeitlin fiber is also more involved in this case. We start by canonically decomposing an orthogonal GZ fiber as a product $F_U \times F_{SO}$, where F_U behaves like a unitary GZ fiber, and the rest of the section is dedicated to examining F_{SO} .

Notation 5.1. As a matter of convenience, we extend the diagram of Figure 3 for an orthogonal Gelfand–Zeitlin fiber, which conventionally starts with $a = 2$, to $a = 1$ by taking $G_k = H_k = L_k = SO(1)$ and setting $F^k = F_1^k$. We write $F = F^{n+1}$ for the Gelfand–Zeitlin fiber itself. In the product decomposition given by Corollary 3.3, we write F_U for the product of the factors corresponding to white components in the corresponding Gelfand–Zeitlin pattern and F_{SO} for the product of the factors corresponding to white components. Hence $F \cong F_U \times F_{SO}$.

Decomposing H_k and L_k respectively as $H_k^U \times H_k^{SO}$ and $L_k^U \times L_k^{SO}$ with H_k^U and L_k^U products of unitary groups and H_k^{SO} and L_k^{SO} orthogonal, both F_U and F_{SO} admit tower descriptions as in Figure 3, given by taking F_k^k and F_k^{k+1} to respectively be $SO(k)/H_k^U$ and $SO(k)/L_k^U$ in the former case and $SO(k)/H_k^{SO}$ and $SO(k)/L_k^{SO}$ in the latter.

Because the quotients H_k^U/L_k^U are products of odd-dimensional spheres, the proof of Theorem 4.1 again applies to give the following.

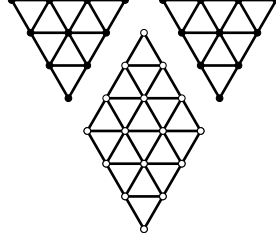
Theorem 5.2. *Given an orthogonal Gelfand–Zeitlin fiber F , the cohomology ring $H^*(F_U; \mathbb{Z})$ is an exterior algebra $\Lambda[z_{2d-1,i}]$, where the generators $z_{2d-1,i}$ of degree $2d - 1$ are enumerated by black Δ -shapes of width d in the positive part of the Gelfand–Zeitlin pattern.*

By the same reasoning as in Remark 4.5, one has the following; one similarly has analogues of Remark 4.5 and Propositions 4.6 and 4.7.

Proposition 5.3. *Given an orthogonal Gelfand–Zeitlin fiber F , the factor F_U is itself the product of a torus T and a space Y with $\pi_1(Y) = 0 = \pi_2(Y)$. The dimension of T is the number of Δ -shapes of width 1 in the positive part of the Gelfand–Zeitlin pattern.*

Since $H^*(F_U)$ is free abelian, the Künneth theorem shows $H^*(F)$ is isomorphic as a graded ring to $H(F_U) \otimes H^*(F_{SO})$, so we focus exclusively on F_{SO} for the rest of the section.

Example 5.4. Following Examples 3.13 and 3.14, we see the GZ fiber F^8 associated to the orthogonal GZ pattern



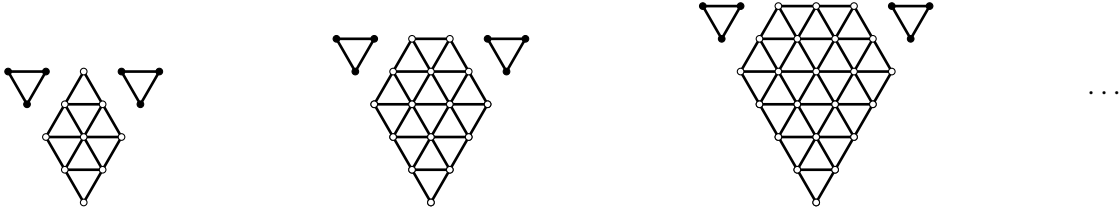
can be identified with $SO(4)$. Its cohomology rings over \mathbb{Z} and $\mathbb{Z}[1/2]$ are respectively

$$\frac{\mathbb{Z}[s] \otimes \Lambda[z, q]}{(2y, y^2, sq)} \quad \text{and} \quad \Lambda[z, q],$$

where $|y| = 2$ and $|z| = |q| = 3$. Larger “diamond and two triangle” patterns give GZ fibers diffeomorphic to $SO(k)$, for any k , hence any description of the cohomology of an orthogonal GZ fiber must be at least as complex as the corresponding description for $SO(k)$. The integral cohomology ring of $SO(k)$ has been known in full only since the late 1980s and its description is involved [Pit91].

One can also encounter 2-torsion in the fiber in other ways.

Example 5.5. Consider the following family of orthogonal GZ patterns.



From Example 3.16 we see the member of the series where the white component has width m corresponds to a GZ fiber diffeomorphic to the Stiefel manifold $V_2(\mathbb{R}^m) = SO(m)/SO(m-2)$. The first three, pictured above, respectively give $SO(3)$, $SO(4)/SO(2)$, and $SO(5)/SO(3)$. We single out this sequence of examples because it gives the simplest instances of nontrivial differentials in spectral sequences associated to orthogonal GZ patterns. The projection $SO(m)/SO(m-2) \rightarrow SO(m)/SO(m-1) = S^{m-1}$ with fiber $SO(m-1)/SO(m-2) = S^{m-1}$ displays $V_2(\mathbb{R}^m)$ as the total space of the unit sphere subbundle of the tangent bundle of S^{m-1} , whose associated Serre spectral sequence can support a nontrivial differential d_{m-1} as in Figure 6.

One has $d_{m-1}z = \chi(S^{m-1})s$, where the Euler characteristic $\chi(S^{m-1})$ is $1 + (-1)^{m-1}$, so the differential is zero when m is even but $2s$ when m is odd. There is no extension problem because each diagonal file of the E_∞ page contains only one nonzero entry, so the cohomology ring structure for $V_2(\mathbb{R}^m)$ follows entirely from degree considerations and Poincaré duality. When m is even, one finds $H^*(V_2(\mathbb{R}^m)) \cong \Lambda[z, s]$, with arbitrary coefficients, whereas when $m = 2k + 1$ is odd, the cohomology rings over \mathbb{Z} and $\mathbb{Z}[1/2]$ are respectively

$$\frac{\mathbb{Z}[s] \otimes \Lambda[z]}{(2s, s^2, sz)}, \quad |s| = 2k, \quad |z| = 2k - 1 \quad \text{and} \quad \Lambda[q], \quad |q| = 4k - 1.$$

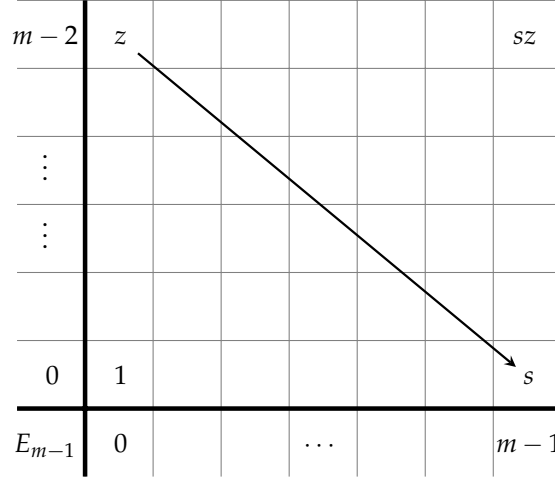


Figure 6: The differential d_{m-1} in the Serre spectral sequence of $S^{m-1} \rightarrow V_2(\mathbb{R}^m) \rightarrow S^m$.

In general, there exists a complete presentation for the ring $H^*V_k(\mathbb{R}^m)$ due to Čadek, Mimura, and Vanžura [ČaMV03], which is rather complicated and includes Pittie’s presentation [Pit91] of $H^*\text{SO}(m)$ as the $k = m - 1$ case.

These examples are meant to indicate it is probably unduly optimistic to expect a closed form for the integral cohomology ring of F_{SO} , but that the cohomology ring modulo torsion, mod-2 cohomology ring and the cohomology groups over \mathbb{Z} should still be accessible.

Notation 5.7. In the Bockstein long exact sequence of cohomology groups of a space X arising from the short exact sequence $0 \rightarrow \mathbb{Z} \rightarrow \mathbb{Z} \rightarrow \mathbb{Z}/2 \rightarrow 0$ of coefficient rings, we write $\beta: H^{*-1}(X; \mathbb{F}_2) \rightarrow H^*(X)$ for the connecting map and $\rho: H^*(X) \rightarrow H^*(X; \mathbb{F}_2)$ for the reduction map, which is a ring homomorphism. The first Steenrod square is $\text{Sq}^1 = \rho\beta: H^{*-1}(X; \mathbb{F}_2) \rightarrow H^*(X; \mathbb{F}_2)$. We also write $\overline{H^*(X)} = H^*(X)/\text{torsion}$.

These maps are used essentially in the determination of the cohomology rings of $\text{SO}(m)$ and $V_k(\mathbb{R}^m)$, as referenced in Examples 5.4 and 5.5, which have torsion only of order 2. We will need some algebraic terminology for the partial description we give.

Definition 5.8. Let k be \mathbb{Z} or a finite quotient thereof, A a commutative graded algebra, and M a submodule of A free over k . We say M *admits a simple system of generators* if there are elements $v_j \in M$ such that the distinct monomials $v_{j_1} \cdots v_{j_\ell}$ of degree 0 or 1 in each v_j form a k -basis of M . If A itself admits a simple system of generators, then its ring structure is determined entirely by the existence of the simple system of generators and the values of the squares v_j^2 .⁵

Proposition 5.9 (Čadek–Mimura–Vanžura [ČaMV03]). *The cohomology ring $H^*(\text{SO}(M)/\text{SO}(m); \mathbb{F}_2)$ admits a system of one simple generator v_i of each degree $i \in [m, M - 1]$ with $v_i^2 = v_{2i}$ for $2i < M$ and $v_i^2 = 0$ for $2i \geq M$ and $\text{Sq}^1 v_{2i} = v_{2i+1}$ for $2i + 1 < M$. All torsion in $H^*(\text{SO}(M)/\text{SO}(m))$ is 2-torsion and the torsion ideal has a canonical free abelian complement admitting a simple system of generators. This simple system consists of the following nontorsion generators indexed by degree:*

$$q_{4j-1} \quad \text{whenever } [2j - 1, 2j + 1] \subseteq [m, M], \quad u_m \quad \text{if } m \text{ is even}, \quad \chi_{2\ell-1} \quad \text{if } M = 2\ell.$$

⁵ For example, the polynomial ring $\mathbb{Z}[x]$ admits the simple system of generators x^{2^j} despite not being exterior.

The square of these generators are 2-torsion, and particularly the squares u_m^2 and $\chi_{2\ell-1}^2$ are 0.

One has $\rho\chi_{2\ell-1} = v_{2\ell-1}$. Given $N < M$, the maps induced by the inclusion $\mathrm{SO}(N)/\mathrm{SO}(m) \rightarrow \mathrm{SO}(M)/\mathrm{SO}(m)$ are surjective on the v_i , the q_{4j-1} , and u_m , but $\chi_{2\ell-1}$ is not in the image. When $M = 2\ell$ is even and $M > n > m$, the map induced in cohomology by the quotient map $\mathrm{SO}(M)/\mathrm{SO}(m) \rightarrow \mathrm{SO}(M)/\mathrm{SO}(n)$ does preserve $\chi_{2\ell-1}$. The transgression of $\chi_{2\ell-1}$ in the Serre spectral sequence of the universal principal $\mathrm{SO}(2\ell)$ -bundle is a non-torsion class $e_{2\ell} \in H^{2\ell} \mathrm{BSO}(2\ell)$, the **Euler class**, which is annihilated by restriction along the maps $\mathrm{BSO}(N) \rightarrow \mathrm{BSO}(2\ell)$ for $N < 2\ell$.

We will show that, similarly, both $\overline{H^*(F_{\mathrm{SO}})}$ and $H^*(F_{\mathrm{SO}}; \mathbb{F}_2)$ admit simple systems of generators and $H^*(F_{\mathrm{SO}})$ has only 2-torsion. To state the result precisely it will help to expand our graphical lexicon.

Notation 5.10. We refer to as a $\mathbf{\Delta}$ -shape any three consecutive rows $k, k+1, k+2$ in an orthogonal Gelfand–Zeitlin pattern such that the full subgraph on the white components in these rows is made up of a Δ -shape in rows k and $k+1$ and an Δ -shape in rows $k+1$ and $k+2$. For example, there is precisely one $\mathbf{\Delta}$ -shape in each member of the family in Example 5.5.

For either of the shapes Δ and $\mathbf{\Delta}$, we will use subscript labels to refer to the width ℓ , counted in vertices, of the bottom row of the shape, or the parity $\bar{\ell} = \ell \bmod 2$ of this width. For instance, the pattern in Example 5.4 has a Δ_0 -shape, more specifically a Δ_4 -shape, in rows 4 and 5, and a $\mathbf{\Delta}_3$ -shape above in rows 5, 6, 7.

We refer to as a (white) \square -shape the full subgraph of a white component of an orthogonal Gelfand–Zeitlin pattern bounded by (and including) two rows whose widths are consecutive local maxima. If the top row is of locally maximum width, it *does not count* as a hexagon. For example, in the patterns in Examples 5.4 and 5.5, there is precisely one \square -shape, in Figure 17 there is one (the white vertex in the top row does not count), and in coming Figure 13 there are five. To a \square -shape of width M vertices at its longest row and m vertices at its top row, we assign the *associated Stiefel manifold* $\mathrm{SO}(M)/\mathrm{SO}(m) = V_{M-m}(\mathbb{R}^M)$. For example in the family in Example 5.5, the \square -shapes are assigned $V_2(\mathbb{R}^3)$, $V_2(\mathbb{R}^4)$, $V_2(\mathbb{R}^5)$, etc., and in Example 5.4, the \square -shape is assigned $\mathrm{SO}(4)/\mathrm{SO}(1) \cong \mathrm{SO}(4)$.

Theorem 5.11. *In the cohomology of the component F_{SO} of an orthogonal Gelfand–Zeitlin fiber as defined in Notation 5.1, all torsion is 2-torsion. If V_p are the Stiefel manifolds associated to the white \square -shapes of the Gelfand–Zeitlin-pattern in Notation 5.10, one has graded group isomorphisms*

$$H^*(F_{\mathrm{SO}}) \cong H^*\left(\prod_{p=1}^r V_p\right) \quad \text{and} \quad H^*(F_{\mathrm{SO}}; \mathbb{F}_2) \cong \bigotimes_{p=1}^r H^*(V_p; \mathbb{F}_2)$$

and a graded ring isomorphism

$$\overline{H^*(F_{\mathrm{SO}})} \cong \bigotimes \overline{H^*(V_p)} \cong \Lambda[z_{s_i}, q_{4s'_j-1}], \quad |z_{s_i}| = s_i, \quad |q_{4s'_j-1}| = 4s'_j - 1,$$

where the generators $q_{4s'_j-1}$ are indexed by the white $\mathbf{\Delta}_{2s'_j+1}$ -shapes in the Gelfand–Zeitlin pattern and the generators z_{s_i} are indexed by the set of those white Δ_{s_i+1} -shapes not contained in any $\mathbf{\Delta}_1$ -shape.⁶

Before diving into the proof, we give an example.

⁶ For ease of presentation, we allow even-dimensional exterior generators, meaning central elements squaring to 0.

Example 5.12. Consider an orthogonal GZ pattern with white component outlined in Figure 13, where rows of locally maximal or minimal width are labeled by their widths. One has an expression $F_{SO}^{22} \cong X \otimes_{SO(1)} Y = X \times Y$, where X and Y are the spaces corresponding to the subpatterns joined at the pinch point of width 1.

Counting \mathbf{A}_1 -shapes, we find a \mathbf{A}_3 -shape (a triangle) contributing a $V_2(\mathbb{R}^3) = SO(3)$ factor in cohomology and a disjoint \mathbf{A}_3 -shape contributing an S^2 factor. Counting all \mathbf{A} -shapes, we find two \mathbf{A}_3 's and an \mathbf{A}_2 , so $H^*(X; \mathbb{F}_2)$ admits a simple system of generators of orders 2, 2, 1. For the ring structure, the balanced product description

$$X \cong SO(1) \otimes_{SO(1)} SO(3) \otimes_{SO(2)} SO(3)/SO(1) \cong SO(3) \otimes_{SO(2)} SO(3).$$

gives the sequence of Stiefel manifolds $SO(3)/SO(2) \cong S^2$ and $SO(3)/SO(1) \cong SO(3)$ corresponding to the \mathbf{A} -shapes. In this case the diffeomorphism $g \otimes h \mapsto (gSO(2), gh)$ gives us $S^2 \times SO(3)$.

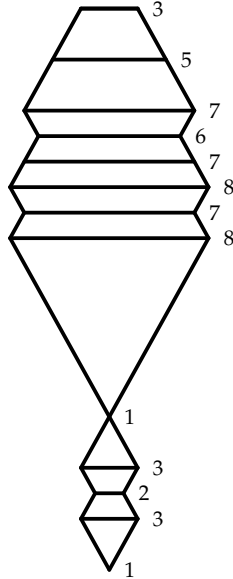


Figure 13: Outline of a white component of a GZ pattern on a non-regular coadjoint orbit of $SO(22)$; the numerical labels are row width in number of vertices.

Similarly, reading up from the bottom of the other component Y for \mathbf{A} -shapes, we find the Stiefel manifolds $S^7 \cong SO(8)/SO(7)$, $V_2 = SO(8)/SO(6)$, and $V_3 = SO(7)/SO(3)$. In the balanced product description

$$Y \cong SO(1) \otimes_{SO(1)} SO(8) \otimes_{SO(7)} SO(8) \otimes_{SO(6)} SO(7)/SO(3),$$

the first Stiefel manifold S^7 splits off to leave $SO(8) \otimes_{SO(6)} SO(7)/SO(3)$, a V_3 -bundle over V_2 . Reading the remaining two \mathbf{A} -shapes, corresponding to V_2 and V_3 , for \mathbf{A} -shapes, we find a \mathbf{A}_7 and a \mathbf{A}_5 , respectively giving factors $H^*V_2(\mathbb{R}^7)$ and $H^*V_2(\mathbb{R}^5)$. Then looking for \mathbf{A} -shapes not contained in these, one encounters, reading from the bottom, two \mathbf{A}_8 's and a \mathbf{A}_7 , respectively contributing two S^7 factors and an S^6 . Thus Y has the cohomology of $S^7 \times S^7 \times S^6 \times V_2(\mathbb{R}^7) \times V_2(\mathbb{R}^5)$ additively over \mathbb{Z} and \mathbb{F}_2 , and multiplicatively over \mathbb{Z} after quotienting out 2-torsion.

Proof of Theorem 5.11. Indexing the V_p in increasing order from the bottom of the pattern, the expression (3.7) shows F_{SO} is the total space in the tower

$$\begin{array}{ccccccccc}
 V_r & & V_{r-1} & & V_{r-2} & & \cdots & & V_3 & & V_2 \\
 \downarrow i_r & & \downarrow i_{r-1} & & \downarrow i_{r-2} & & & & \downarrow i_3 & & \downarrow i_2 \\
 F_{\text{SO}} & \longrightarrow & F^{\ell_{r-1}} & \longrightarrow & F^{\ell_{r-2}} & \longrightarrow & \cdots & \longrightarrow & F^{\ell_3} & \longrightarrow & F^{\ell_2} & \longrightarrow & V_1,
 \end{array} \tag{5.14}$$

with

$$F^{\ell_p} = \text{SO}(M_1) \otimes_{\text{SO}(m_1)} \text{SO}(M_2) \otimes_{\text{SO}(m_2)} \cdots \otimes_{\text{SO}(m_{p-1})} \text{SO}(M_p)/\text{SO}(m_p) \tag{5.15}$$

and fiber inclusions $i_p: \text{SO}(M_p)/\text{SO}(m_p) = V_p \rightarrow F^{\ell_p}$ given by $g_p \text{SO}(m_p) \mapsto 1 \otimes \cdots \otimes 1 \otimes g_p \text{SO}(m_p)$.

We show the associated rational and mod-2 Serre spectral sequences collapse. Fix $p \in [1, r]$. Letting N be the largest of the M_t for $t \in [1, p]$, we observe that $\prod_t \text{SO}(M_t)$ is a subgroup of $\text{SO}(M)^\rho$, where $M_{\ell_r} = 2\ell$, and that the iterated group multiplication $(g_1, \dots, g_p) \mapsto g_1 \cdots g_p$ on $\text{SO}(N)$ restricts to a map $\prod_t \text{SO}(M_t) \rightarrow \text{SO}(N)$. By the definition of the balanced product, this multiplication descends to a well-defined map

$$\begin{aligned}
 \mu_p: F^{\ell_p} &\longrightarrow \text{SO}(N)/\text{SO}(m_p), \\
 g_1 \otimes \cdots \otimes g_p \text{SO}(m_p) &\longmapsto g_1 \cdots g_p \text{SO}(m_p).
 \end{aligned}$$

It is clear that $\mu_p \circ i_p$ is the standard injection $\text{SO}(M_p)/\text{SO}(m_p) \rightarrow \text{SO}(N)/\text{SO}(m_p)$ we discussed in Proposition 5.9. Thus each generator v_i lies in the image of i_p^* , hence i_p^* is surjective onto $H^*(V_p; \mathbb{F}_2)$ and the mod-2 Serre spectral sequence collapses. This gives the mod-2 isomorphism.

To prove the collapse rationally, note each q_{4j-1} is also in the image of i_p^* , as is u_{m_p} when m_p is even. It remains only to find a lift in $H^{2s-1}(F^{\ell_p})$ of $\chi_{2s-1} \in H^{2s-1}(\text{SO}(M_p)/\text{SO}(m_p))$ if $M_p = 2s$ is even, for which we will need a different map. Abbreviate the balanced product of the first $p-1$ factors in (5.15) as X , so that F^{ℓ_p} is $X \otimes_{\text{SO}(m_{p-1})} \text{SO}(2s)/\text{SO}(m_p)$. There is a quotient map to $F'' = X \otimes_{\text{SO}(m_{p-1})} \text{SO}(2s)/\text{SO}(2s-1)$, and the inclusion i_p then factors through $S^{2s-1} = \text{SO}(2s)/\text{SO}(2s-1)$. As F'' is the orbit space of $X \times \text{SO}(M_p)$ under a free action of $\text{SO}(m_{p-1}) \times \text{SO}(2s-1)$, we may replace $\text{SO}(2s)$ with $S' = \text{ESO}(2s) \times \text{SO}(2s) \times \text{ESO}(2s)$ in its definition and the action by $(h, h') \cdot (x \otimes (e, g, e')) := xh^{-1} \otimes (eh^{-1}, hg(h')^{-1}, h'e')$ to obtain a homotopy-equivalent space F' . Dropping the X coordinate yields a natural quotient map ω to $E \cong \text{ESO}(2s) \otimes_{\text{SO}(m_{p-1})} \text{SO}(2s) \otimes_{\text{SO}(2s-1)} \text{ESO}(2s)$, given by $(x, e) \otimes g \otimes e' \mapsto e \otimes g \otimes e'$. We replace the map $S^{2s-1} \rightarrow F''$ given by $g\text{SO}(2n-1) \mapsto * \otimes g\text{SO}(2n-1)$ with the map $S^{2s-1} \rightarrow F'$ given by $g\text{SO}(2n-1) \mapsto (*, *) \otimes g \otimes *$. These maps then fit together as follows:

$$\begin{array}{ccccc}
 \text{SO}(2s) & \xrightarrow{\pi'} & V_p & \xrightarrow{\pi} & S^{2s-1} \\
 & & \downarrow i_p & & \downarrow i \\
 & & F^{\ell_p} & \xrightarrow{\omega'} & F' & \xrightarrow{\omega} & E.
 \end{array}$$

To lift $\chi_{2s-1} \in H^{2s-1}(V_p)$ to F^{ℓ_p} , it is enough by commutativity of the square to find a lift to F' along $i \circ \pi$. Now by Proposition 5.9, the fundamental class of S^{2s-1} is the unique lift of this element under π^* and also the unique lift of $\tilde{\chi} = (\pi')^* \chi_{2s-1} \in H^* \text{SO}(2s)$ under $(\pi \circ \pi')^*$, so it will be enough to see $\tilde{\chi}$ lies in the image of the fiber restriction $(\omega \circ i \circ \pi \circ \pi')^*$.

For this, we note $\omega \circ i \circ \pi \circ \pi'$ is the fiber inclusion of a nonprincipal $\mathrm{SO}(2s)$ -bundle over $\mathrm{BSO}(m_{p-1}) \times \mathrm{BSO}(2s-1)$ with projection given by $e \otimes g \otimes e' \mapsto (\mathrm{SO}(m_{p-1})e, e'\mathrm{SO}(2s-1))$. We will show that $\tilde{\chi}$ transgresses in the Serre spectral sequence of this bundle, so that it lies in the image of the fiber restriction. Following Eschenburg [Esch92], consider the following square:

$$\begin{array}{ccc}
 E = \mathrm{ESO}(2s) \otimes_{\mathrm{SO}(m_{p-1})} \mathrm{SO}(2s) \otimes_{\mathrm{SO}(2s-1)} \mathrm{ESO}(2s) & \xrightarrow{\tilde{\chi}} & \mathrm{ESO}(2s) \otimes_{\mathrm{SO}(2s)} \mathrm{SO}(2s) \otimes_{\mathrm{SO}(2s)} \mathrm{ESO}(2s) \simeq \mathrm{BSO}(2s) \\
 \downarrow & & \downarrow \\
 \mathrm{BSO}(m_{p-1}) \times \mathrm{BSO}(2s-1) & \xrightarrow{\kappa} & \mathrm{BSO}(2s) \times \mathrm{BSO}(2s).
 \end{array}$$

The right vertical map $e \otimes g \otimes e' \mapsto (\mathrm{SO}(2s)e, e'\mathrm{SO}(2s))$ is the projection of another $\mathrm{SO}(2s)$ -bundle and by inspection the horizontal map $e \otimes g \otimes e' \mapsto e \otimes g \otimes e'$ makes the square a map of $\mathrm{SO}(2s)$ -bundles such that the map κ of base spaces is up to homotopy that induced functorially by the subgroup inclusions. In the Serre spectral sequence of the right bundle, $\tilde{\chi}$ transgresses to the image in $E_{2s}^{2s,0}$ of $1 \otimes e_{2s} - e_{2s-1} \otimes 1 \in H^*\mathrm{BSO}(2s) \otimes H^*\mathrm{BSO}(2s)$, so in the left spectral sequence it transgresses to the $E_{2s}^{2s,0}(\tilde{\kappa})$ -image of this element. But e_{2s} lies in the kernel of $H^*\mathrm{BSO}(2s) \rightarrow H^*\mathrm{BSO}(t)$ for $t < 2s$, by Proposition 5.9, so the map $E_2^{2s,0}(\tilde{\kappa}) = \kappa^* \otimes \mathrm{id}$ already annihilates $1 \otimes e_{2s} - e_{2s-1} \otimes 1$, and $\tilde{\chi}$ transgresses to 0 as claimed. Thus it is the image of some x in $H^{2s-1}(E)$ and our desired lift in $H^{2s-1}(F^{\ell_p})$ is $(\omega \circ \omega')^*x$.

A result of Borel [Bor53, Prop. 8.2] states that given a bundle $F \rightarrow E \rightarrow B$ of compact CW complexes such that all torsion in $H^*(F)$ and $H^*(B)$ is 2-torsion and the rational and mod-2 Serre spectral sequences collapse, the integral spectral sequence also collapses without an extension problem, so that as graded groups, one has $H^*(E) \cong E_\infty = E_2 \cong H^*(B \times F)$. In particular, all torsion in $H^*(E)$ is again 2-torsion, and now the integral result follows by induction. To recover the statement about $H^*(F_{\mathrm{SO}})$, inductively, note that each $\overline{H^*(V_p)}$ is exterior, particularly $\overline{H^*(V_1)}$, and then inductively assume the same of $\overline{H^*(F^{\ell_{p-1}})}$. The Serre spectral sequence of $V_p \rightarrow F^{\ell_p} \rightarrow F^{\ell_{p-1}}$ modulo torsion collapses at $E_2 = \overline{F^{\ell_{p-1}} \otimes H^*(V_p)}$, so it remains to lift a system of exterior generators from $\overline{H^*(V_p)}$. For these we take the various images $\mu_p^* q_{4j-1}$, and additionally $(\omega \circ \omega')^*x$ if M_p is even⁷ and $\mu_p^* u_{m_p}$ if u_{m_p} is even, since $u_{m_p}^2 = 0$ in $H^{2m_p}(\mathrm{SO}(N)/\mathrm{SO}(m_p))$.

The enumeration of generators by trapezoids follows by examining each $V_p = \mathrm{SO}(M_p)/\mathrm{SO}(m_p)$ separately. Write M' for M_p itself if it is odd and otherwise for $M_p - 1$, and similarly m' for m_p itself if it is odd and otherwise for $m_p + 1$. Then there is a bundle tower

$$\begin{array}{ccccccc}
 \frac{\mathrm{SO}(m')}{\mathrm{SO}(m_p)} & \frac{\mathrm{SO}(m'+2)}{\mathrm{SO}(m')} & \frac{\mathrm{SO}(m'+4)}{\mathrm{SO}(m'+2)} & \dots & \frac{\mathrm{SO}(M'-2)}{\mathrm{SO}(M'-4)} & \frac{\mathrm{SO}(M')}{\mathrm{SO}(M'-2)} & \\
 \downarrow & \downarrow & \downarrow & & \downarrow & \downarrow & \\
 V_p & \longrightarrow & \frac{\mathrm{SO}(M_p)}{\mathrm{SO}(m')} & \longrightarrow & \frac{\mathrm{SO}(M_p)}{\mathrm{SO}(m'+2)} & \longrightarrow & \dots & \longrightarrow & \frac{\mathrm{SO}(M_p)}{\mathrm{SO}(M'-4)} & \longrightarrow & \frac{\mathrm{SO}(M_p)}{\mathrm{SO}(M'-2)} & \longrightarrow & \frac{\mathrm{SO}(M_p)}{\mathrm{SO}(M')}.
 \end{array}$$

Borel showed [Bor53, Prop. 10.4] that the cohomology of V_p and of the direct product of the fibers and the base in this diagram are isomorphic. Quotienting out torsion, the cohomology of each fiber and the base space become exterior, on generators, displayed respectively from left to right,

$$\underline{u_{m_p}, \quad q_{2m'+1}, \quad q_{2m'+5}, \quad \dots, \quad q_{2M'-7}, \quad q_{2M'-3}, \quad \chi_{M_p-1}}$$

⁷ Since there is no longer any 2-torsion, for the odd-degree lifts we could really have taken anything.

where u_{m_p} is contributed if and only if the last fiber is nontrivial, which is to say, m_p is even, and χ_{M_p-1} is contributed if and only if the base is nontrivial, which is to say, M_p is even. Now the fibers $\mathrm{SO}(M' - 2t)/\mathrm{SO}(M' - 2t - 2)$ correspond to \mathbf{A} -shapes of (odd) width $M' - 2t$ and $\mathrm{SO}(m')/\mathrm{SO}(m_p)$ and $\mathrm{SO}(M_p)/\mathrm{SO}(M')$ correspond to the possible leftover $\mathbf{\Delta}$ -shapes of respective widths m' and M_p on the top and bottom of the white $\mathbf{\square}$ -shape V_p is associated to. \square

Combining Borel's result [Bor53, Prop. 10.4] and Theorem 5.11, we have an additive characterization that is arguably even simpler.

Corollary 5.16. *In the situation of Theorem 5.11, the graded group $H^*(F_{\mathrm{SO}})$ is isomorphic to the cohomology of a direct product of Stiefel manifolds $V_2(\mathbb{R}^{2s'_j+1})$ indexed by $\mathbf{A}_{2s'_j+1}$ -shapes and of spheres S^{s_i} indexed by $\mathbf{\Delta}_{s_i+1}$ -shapes not contained in any $\mathbf{A}_{\bar{1}}$ -shape.*

We do not hope to give a simple presentation for $H^*(F_{\mathrm{SO}})$ or even $H^*(F_{\mathrm{SO}}; \mathbb{F}_2)$, but we can at least embed the latter as a subring of a better-known ring. Recalling [Bor54, Thm. 8.10] that the Pontrjagin ring of $\mathrm{SO}(n)$ is an exterior algebra on generators, one each in degrees 1 through $n - 1$, dual to the cohomological generators v_i introduced in Proposition 5.9, we have the following by exactly the same reasoning as for Proposition 4.6.

Proposition 5.17. *Let a space X as in (5.15) be given. Then the quotient map*

$$\pi : \prod_{p=1}^r \mathrm{SO}(M_p) \longrightarrow \mathrm{SO}(M_1) \otimes_{\mathrm{SO}(m_1)} \cdots \otimes_{\mathrm{SO}(m_{r-1})} \mathrm{SO}(M_r)/\mathrm{SO}(m_r) = X$$

induces a surjection in mod-2 homology and an identification

$$H_*(X; \mathbb{F}_2) \cong H_*(\mathrm{SO}(M_1); \mathbb{F}_2) \otimes_{H_*(\mathrm{SO}(m_1); \mathbb{F}_2)} \cdots \otimes_{H_*(\mathrm{SO}(m_{r-1}); \mathbb{F}_2)} H_*(\mathrm{SO}(M_r); \mathbb{F}_2) \otimes_{H_*(\mathrm{SO}(m_r); \mathbb{F}_2)} \mathbb{F}_2.$$

Dually, π induces an injection in mod-2 cohomology.

Remark 5.18. One even has π^* an injection integrally if none of the m_p except possibly m_r are even, because the lifts of q_{4j-1} and χ_{2s-1} for $M_p = 2s$ inject under π^* ; but $\pi^*u_{m_p}$ is 2-torsion for m_p even.

Example 5.19. Recall that we promised in Remark 3.17 a counterexample to the most optimistic possible claim about the structure the cohomology ring of $X = \mathrm{SO}(9) \otimes_{\mathrm{SO}(5)} \mathrm{SO}(6)/\mathrm{SO}(2)$. Pulling back along the quotient map μ_1 to $V_1 = \mathrm{SO}(9)/\mathrm{SO}(5)$ we get four generators v'_8, v'_7, v'_6, v'_5 . There is no map to $V_2 = \mathrm{SO}(6)/\mathrm{SO}(2)$, but pulling back along the multiplication map μ_2 to $\mathrm{SO}(9)/\mathrm{SO}(3)$ we get three more generators v''_5, v''_4, v''_3 . These seven classes form a simple system of generators for $H^*(X; \mathbb{F}_2)$ whose respective images in $H^*(\mathrm{SO}(9) \times \mathrm{SO}(6); \mathbb{F}_2)$ under the embedding π^* of Proposition 5.17 are

$$v_8 \otimes 1, \quad v_7 \otimes 1, \quad v_6 \otimes 1, \quad v_5 \otimes 1, \quad v_5 \otimes 1 + 1 \otimes v_5, \quad v_4 \otimes 1 + 1 \otimes v_4, \quad v_3 \otimes 1 + 1 \otimes v_3.$$

In particular, we see $(v''_4)^2 = v'_8$. Since v''_4 lies in the image of μ_2^* but not in that of μ_1^* and v'_8 lies in the image of μ_1^* but not of μ_2^* , there is no way to arrange a ring isomorphism $H^*(F_{\mathrm{SO}}; \mathbb{F}_2) \cong H^*(V_1 \times V_2; \mathbb{F}_2)$.

Integrally, we have a simple system of generators $q'_{15}, q'_{11}, \chi''_5, q''_7$ for the free abelian summand, and in particular $\overline{H^8(F_{\mathrm{SO}})} = 0$. Now $v''_4 = \mathrm{Sq}^1 v''_3 = \rho \beta v''_3$ and $v'_8 = \mathrm{Sq}^1 v'_7 = \rho \beta v'_7$ are reductions of integral classes, and ρ is a ring homomorphism injective on torsion, so it follows that $(\beta v''_3)^2 = \beta v'_7$ in $H^8(F_{\mathrm{SO}})$. Thus we cannot have a ring isomorphism $H^*(F_{\mathrm{SO}}) \cong H^*(V_1 \times V_2)$ either.

We can also use this map π to determine the first three homotopy groups.

Proposition 5.20. *The factor F_{SO} of an orthogonal Gelfand–Zeitlin fiber splits as a direct product of a torus $T \cong \text{SO}(2)^t$ and a space Y with $\pi_1(Y) \cong (\mathbb{Z}/2)^s$ and $\pi_2(Y) \cong \mathbb{Z}^f$ and $\pi_3(Y) \cong \mathbb{Z}^g$, where t , s , and f are determined from the white components of the associated Gelfand–Zeitlin pattern: t is the number of local maxima of width 2, f is the number of local minima of width 2, possibly including the top row, and s is determined by counting the remaining white components remaining after the union of all diamonds of width 2 is deleted, then any resulting component containing 2 or more vertices in the top row is also deleted. We determine g as a sum of numbers h given in terms of the description of factors X as in Proposition 5.17: if N_4 is the number of p such that $M_p = 4$, while $n_{\geq 3}$ is the number with $m_p \geq 3$, then $h = N_4 + r - n_{\geq 3}$.*

Proof. As noted in Example 3.12, each diamond of width 2 contributes an $\text{SO}(2)$ direct factor. Letting T be the product of these, we see each of the remaining components X as described in Proposition 5.17 satisfies $M_p \geq 3$, with all $m_p \geq 2$ except possibly m_r . As Y is the product of these X , it suffices to examine each X separately. Since π_2 of a Lie group is trivial, the homotopy long exact sequence associated to the map π from Proposition 5.17 gives $0 \rightarrow \pi_2(X) \rightarrow \prod \pi_1 \text{SO}(m_p) \rightarrow \prod \pi_1 \text{SO}(M_p) \rightarrow \pi_1(X) \rightarrow 0$. Since the subgroup inclusion $\text{SO}(m) \hookrightarrow \text{SO}(n)$ induces an isomorphism on $\pi_1 \cong \mathbb{Z}/2$ for $m \geq 3$ and the surjection $\mathbb{Z} \rightarrow \mathbb{Z}/2$ for $m = 2$, and each M_p is at least 3, the central map factors through the reduction mod 2, whose kernel is a direct product of f copies of $2\mathbb{Z} < \mathbb{Z} = \pi_1 \text{SO}(2)$, one per index p with $m_p = 2$. This will show $\pi_2(X) \cong \mathbb{Z}^f$ once we see the second factor is injective, but this map takes $(a, b, \dots, x, y) \in (\mathbb{Z}/2)^{r-1}$ to $(a, a+b, \dots, x+y, y) \in (\mathbb{Z}/2)^r$ if $m_r \leq 1$ and otherwise takes $(a, b, \dots, x, y, z) \in (\mathbb{Z}/2)^r$ to $(a, a+b, \dots, x+y, y+z) \in (\mathbb{Z}/2)^r$. It is thus injective either way, with cokernel $\pi_1(X)$ isomorphic to $\mathbb{Z}/2$ in the former case and to 0 in the latter.

As for $\pi_3(X)$, the triviality of $\prod \pi_2 \text{SO}(m_p)$ again gives a cokernel expression

$$\pi_3(X) \cong \pi_3 \text{SO}(M_1) \otimes_{\pi_3 \text{SO}(m_1)} \cdots \otimes_{\pi_3 \text{SO}(m_{r-1})} \pi_3 \text{SO}(M_r) \otimes_{\pi_3 \text{SO}(m_r)} 0.$$

Now recall that $\pi_3 \text{SO}(2) = 0$, while $\pi_3 \text{SO}(4) \cong \mathbb{Z}^2$ and for all other $m \geq 3$ we have $\pi_3 \text{SO}(m) \cong \mathbb{Z}$, with the image of $\pi_3 \text{SO}(m) \rightarrow \pi_3 \text{SO}(n)$ isomorphic to \mathbb{Z} for all $n \geq m \geq 3$. It follows that a p such that $M_p = 4$ contributes two \mathbb{Z} summands, while a p such that $4 \neq M_p \geq 3$ contributes just one, and any p such that $m_p \geq 3$ cancels one summand, since only one of the sets $\{M_p, M_{p+1}\}$ and $\{m_p\}$ can contain 4. \square

Remark 5.21. The description of a GZ fiber as a product of biquotients (hence a biquotient itself) from Theorem 3.8 makes available a different closed-form expression for the cohomology of such spaces. Singhof [Sing93] observed that a biquotient $K \backslash G / H$ of compact, connected Lie groups can be expressed up to homotopy as the homotopy pullback of the diagram $BK \rightarrow BG \leftarrow BH$, to which Munkholm’s general Eilenberg–Moore collapse result [Munk74] applies to yield

$$H^*(K \backslash G / H; k) \cong \text{Tor}_{H^*(BG; k)}^*(H^*(BK; k), H^*(BH; k)) \quad (5.22)$$

as graded modules over any principal ideal domain k of characteristic $\neq 2$ such that the cohomology rings of BG , BK , BH are polynomial. Vitali Kapovitch [Kap04], building on work of Eschenburg [Esch92], showed (5.22) holds as a ring isomorphism for $k = \mathbb{Q}$, and the first author recently found, using A_∞ -algebraic techniques and a product due to Franz on a two-sided bar construction, that (5.22) is a multiplicative so long as 2 is a unit of k [CF21].

Since $H^*U(n)$ is free abelian and $H^*SO(n)$ has torsion only of order two, (5.22) determines the cohomology ring of any unitary or orthogonal GZ fiber for $k = \mathbb{Z}[1/2]$. For a general biquotient, knowing (5.22) greatly simplifies life since the Tor in question is algorithmically computable using with a finitely generated Koszul complex, but in the present case, it is easier still to simply read the ring structure off the GZ pattern.

References

- [Ala09] I. Alamiddine. *Géométrie de systèmes hamiltoniens intégrables: Le cas du système de Gelfand-Ceitlin*. PhD thesis, Université Toulouse, 2009. <http://thesesups.ups-tlse.fr/538>.
- [BMMT18] A. Bolsinov, V. S. Matveev, E. Miranda, and S. Tabachnikov. Open problems, questions and challenges in finite-dimensional integrable systems. *Philos. Trans. Roy. Soc. A*, 376, 2018. [arXiv:1804.03737](https://arxiv.org/abs/1804.03737), [doi:10.1098/rsta.2017.0430](https://doi.org/10.1098/rsta.2017.0430).
- [Bor53] A. Borel. Sur la cohomologie des espaces fibrés principaux et des espaces homogènes de groupes de Lie compacts. *Ann. of Math. (2)*, 57(1):115–207, 1953. [doi:10.2307/1969728](https://doi.org/10.2307/1969728), <http://web.math.rochester.edu/people/faculty/doug/otherpapers/Borel-Sur.pdf>.
- [Bor54] Armand Borel. Sur l’homologie et la cohomologie des groupes de Lie compacts connexes. *American J. Math.*, pages 273–342, 1954. [doi:10.2307/2372574](https://doi.org/10.2307/2372574).
- [Bou18] D. Bouloc. Singular fibers of the bending flows on the moduli space of 3D polygons. *J. Symplectic Geom.*, 16(3):585 – 629, 2018. [arXiv:1505.04748](https://arxiv.org/abs/1505.04748), [doi:10.4310/JSG.2018.v16.n3.a1](https://doi.org/10.4310/JSG.2018.v16.n3.a1).
- [BouMZ18] D. Bouloc, E. Miranda, and N. T. Zung. Singular fibers of the Gelfand-Cetlin system on $u(n)^*$. *Philos. Trans. Roy. Soc. A*, 376, 2018. [arXiv:1803.08332](https://arxiv.org/abs/1803.08332), [doi:10.1098/rsta.2017.0423](https://doi.org/10.1098/rsta.2017.0423).
- [ČaMV03] M. Čadek, M. Mimura, and J. Vanžura. The cohomology rings of real Stiefel manifolds with integer coefficients. *J. Math. Kyoto Univ.*, 43(2):411–428, 2003. [doi:10.1215/kjm/1250283733](https://doi.org/10.1215/kjm/1250283733).
- [CF21] J. D. Carlson (appendix joint with M. Franz). The cohomology of biquotients via a product on the two-sided bar construction (expository version). 2021. [arXiv:2106.02986](https://arxiv.org/abs/2106.02986).
- [CK20] Y. Cho and Y. Kim. Lagrangian fibers of Gelfand–Cetlin systems of $SO(n)$ -type. *Transform. Groups*, May 2020. [arXiv:1806.01529](https://arxiv.org/abs/1806.01529), [doi:10.1007/s00031-020-09566-4](https://doi.org/10.1007/s00031-020-09566-4).
- [CKO20] Y. Cho, Y. Kim, and Y.-G. Oh. Lagrangian fibers of Gelfand–Cetlin systems. *Adv. Math.*, 372, 2020. [arXiv:1911.04132](https://arxiv.org/abs/1911.04132), [doi:10.1016/j.aim.2020.107304](https://doi.org/10.1016/j.aim.2020.107304).
- [Esch92] J.-H. Eschenburg. Cohomology of biquotients. *Manuscripta Math.*, 75(2):151–166, 1992. [doi:10.1007/BF02567078](https://doi.org/10.1007/BF02567078).
- [Gold86] W. M. Goldman. Invariant functions on Lie groups and Hamiltonian flows of surface group representations. *Invent. Math.*, 85(2):263–302, June 1986. [doi:10.1007/BF01389091](https://doi.org/10.1007/BF01389091).
- [GS83a] V. Guillemin and S. Sternberg. The Gelfand–Cetlin system and quantization of the complex flag manifolds. *J. Funct. Anal.*, 52(1):106–128, 1983. [doi:10.1016/0022-1236\(83\)90092-7](https://doi.org/10.1016/0022-1236(83)90092-7).
- [GS83b] V. Guillemin and S. Sternberg. On collective complete integrability according to the method of Thimm. *Ergodic Theory Dynam. Systems*, 3(2):219–230, 1983. [doi:10.1017/S0143385700001930](https://doi.org/10.1017/S0143385700001930).
- [HK14] M. D. Hamilton and H. Konno. Convergence of Kähler to real polarizations on flag manifolds via toric degenerations. *J. Symplectic Geom.*, 12(3):473–509, September 2014. [arXiv:1105.0741](https://arxiv.org/abs/1105.0741), [doi:10.4310/JSG.2014.v12.n3.a3](https://doi.org/10.4310/JSG.2014.v12.n3.a3).
- [HK15] M. Harada and K. Kaveh. Integrable systems, toric degenerations and Okounkov bodies. *Invent. Math.*, 202(3):927–985, 2015. [doi:10.1007/s00222-014-0574-4](https://doi.org/10.1007/s00222-014-0574-4).
- [HL20] B. Hoffman and J. Lane. Stratified gradient Hamiltonian vector fields and collective integrable systems. October 2020. [arXiv:2008.13656](https://arxiv.org/abs/2008.13656).
- [KaKLS20] S. Kaji, S. Kuroki, E. Lee, and D. Y. Suh. Flag Bott manifolds of general Lie type and their equivariant cohomology rings. *Homology Homotopy Appl.*, 22(1):375–390, 2020. [arXiv:1905.00303](https://arxiv.org/abs/1905.00303), [doi:10.4310/HHA.2020.v22.n1.a21](https://doi.org/10.4310/HHA.2020.v22.n1.a21).

- [Kap04] V. Kapovitch. A note on rational homotopy of biquotients. 2004. <http://math.toronto.edu/vtk/biquotient.pdf>.
- [KapM96] M. Kapovich and J. Millson. The symplectic geometry of polygons in Euclidean space. *J. Differential Geom.*, 44(3):479–513, 1996.
- [Lane18] J. Lane. Convexity and Thimm’s trick. *Transform, Groups*, 23:963 – 987, 2018. [arXiv:1509.07356](https://arxiv.org/abs/1509.07356), [doi:10.1007/s00031-017-9436-7](https://doi.org/10.1007/s00031-017-9436-7).
- [Munk74] Hans J. Munkholm. The Eilenberg–Moore spectral sequence and strongly homotopy multiplicative maps. *J. Pure Appl. Algebra*, 5(1):1–50, 1974. [doi:10.1016/0022-4049\(74\)90002-4](https://doi.org/10.1016/0022-4049(74)90002-4).
- [NNU10] T. Nishinou, Y. Nohara, and K. Ueda. Toric degenerations of Gelfand–Cetlin systems and potential functions. *Adv. Math.*, 224(2), 2010. [arXiv:0810.3470](https://arxiv.org/abs/0810.3470), [doi:10.1016/j.aim.2009.12.012](https://doi.org/10.1016/j.aim.2009.12.012).
- [NU16] Y. Nohara and K. Ueda. Floer cohomologies of non-torus fibers of the Gelfand–Cetlin system. *J. Symplectic Geom.*, 14(4):1251–1293, 2016. [arXiv:1409.4049](https://arxiv.org/abs/1409.4049), [doi:10.4310/JSG.2016.v14.n4.a9](https://doi.org/10.4310/JSG.2016.v14.n4.a9).
- [Pab12] M. Pabiniak. *Hamiltonian Torus Actions in Equivariant Cohomology and Symplectic Topology*. PhD thesis, Cornell University, 2012. <http://pi.math.cornell.edu/~milena/thesis.pdf>.
- [Pit91] H. V. Pittie. The integral homology and cohomology rings of $SO(n)$ and $Spin(n)$. *J. Pure Appl. Algebra*, 73(2):105–153, 1991. [doi:10.1016/0022-4049\(91\)90108-E](https://doi.org/10.1016/0022-4049(91)90108-E).
- [Sing93] W. Singhof. On the topology of double coset manifolds. *Math. Ann.*, 297(1):133–146, 1993. [doi:10.1007/BF01459492](https://doi.org/10.1007/BF01459492).

DEPARTMENT OF MATHEMATICS,
IMPERIAL COLLEGE LONDON
j.carlson@imperial.ac.uk

DEPARTMENT OF MATHEMATICS & STATISTICS,
MCMMASTER UNIVERSITY
lanej5@math.mcmaster.ca